Journal of Forestry, 2024, **XX**, 1–19
https://doi.org/10.1093/jofore/fvae020
Advance access publication 2 September 2024
Research Article

OXFORD

Do Experimental Forests and Ranges of the Southeastern United States Represent the Climate, Ecosystem Structure, and Ecosystem Functions of the Region?

Jingfeng Xiao[1,*], Ge Sun[2,*] Kevin M. Potter[2], Johnny Boggs[2] Qingyuan Zhang[3], and Steven G. McNulty[2]

[1]Earth Systems Research Center, Institute for the Study of Earth, Oceans, and Space, University of New Hampshire, Durham, NH, 03824, USA.
[2]Eastern Forest Environmental Threat Assessment Center, Southern Research Station, USDA Forest Service, Research Triangle Park, NC, 27709, USA.
[3]Cooperative Institute for Satellite Earth System Studies, Earth System Science Interdisciplinary Center, University of Maryland, College Park, MD, 20740, USA.

[*]Corresponding authors email: j.xiao@unh.edu. Ge Sun: email: ge.sun@usda.gov

Abstract

There are twenty experimental forest and range sites (EFRs) across the southeastern United States that are currently maintained by the USDA Forest Service (Forest Service) to conduct forest ecosystem research for addressing ecosystem management challenges. The overall objective of this study was to use multiple gridded datasets to assess the extent to which the twenty EFRs represent the climate, ecosystem structure, and ecosystem functions of southeastern forests. The EFRs represent the large variability of climate conditions across the region relatively well, but we identified small representation gaps. The representativeness of ecosystem structure by these EFRs can be improved by establishing EFRs in forests with relatively low tree cover, leaf area index, or tree canopy height. The current EFRs also represent the forest ecosystem functions of the region relatively well, although areas with intermediate and low aboveground biomass and water yield are not well represented. The trends in climate, ecosystem structure, and ecosystem functions were generally consistent between the region and the EFRs. Our study indicates that the current EFRs represent the region relatively well, but establishing additional EFRs in specific areas within the region could help more completely assess how southeastern forests respond to climate change, disturbance, and management practices.

Study Implications: This study across the experimental forests and ranges (EFRs) and the southeastern forest region fills the knowledge gap regarding climate, ecosystem structure, and ecosystem functions of EFRs in the context of the broader southeastern forest region. Understanding ecosystem functions and structures across the EFR network can help the Southern Research Station to address new research questions. Our study indicates that the current EFRs represent the climate, ecosystem structure, and ecosystem functions of southeastern forests well. However, establishing additional EFRs in certain regions could help more completely assess how southeastern forests respond to climate change, disturbance, and management practices.

Keywords: southern forests, experimental forests, ecosystem services, satellite data, representativeness

Introduction

The southeastern forest region of the United States stretches from Texas across to Virginia, from Kentucky down to Florida, and from Oklahoma in the West to North Carolina in the East. Southeastern forests provide important ecosystem services such as timber supply, carbon sequestration, and water supplies, and benefit human health and well-being (Aguilos et al. 2020; Liu et al. 2020; Sun et al. 2005, 2008; Xiao et al. 2011). For example, the southeastern forest region is the "wood basket" of the nation; southeastern forests account for only 2% of the world's forest area but produce 63% of the US timber harvest by volume (Oswalt et al. 2014) and 18% of the world's pulpwood for paper (World Resources Institute 2010). Over 50% of people in the eastern US (57 million) depend on forests for their drinking water supply (Liu et al. 2020). The southeastern forest region also has the most biodiversity (e.g., plant families, amphibians, and freshwater fish) in the nation by some measures (Stein et al. 2000) due to warm temperatures, abundant precipitation, and high ecosystem productivity. Disturbances such as extreme droughts and hurricanes have substantial impacts on southeastern forest ecosystems (Chambers et al. 2007; McNulty 2002; Williams et al. 2017; Xiao et al. 2011), leading to reduced forest productivity and a loss of carbon stocks. These same disturbances, which are expected to increase in the region during the twenty-first century, can also increase insect and disease outbreaks and wildfires (Hoffman et al. 2023).

The USDA Forest Service (FS) has a national network of eighty long-term experimental areas (also known as experimental forests and ranges [EFRs]) dating back to 1908 (Stine 2016). The EFRs represent the largest and longest continuous ecological research network in the United States (USDA FS

Received: January 24, 2024. **Accepted:** July 9, 2024.

2023). The EFRs have been used to support research in studying how land management affects water quality and quantity; how to manage and restore forests and watersheds; how carbon stocks/fluxes and water regulation changes in the context of climate change and management; and how fire, insects, invasive species, and other disturbances affect the health of forests. Some of these forests provide real-time data on climate, hydrology, and biology for researchers, managers, and educators (USDA FS 2023). The Southern Research Station (SRS) EFR Network consists of twenty EFRs, including nineteen official EFRs and one cooperating EFR, which are distributed across the southeastern forest region (figure 1; Table 1). Each EFR is dominated by a specific forest or ecosystem type. For example, the Escambia EFR, located in southern Alabama, and the Palustris EFR, located in central Louisiana, support longleaf pine (*Pinus palustris*) restoration, management, and physiology studies. The Coweeta Hydrologic Laboratory EFR, located in Otto, North Carolia, is the world's oldest forest hydrology research laboratory (Nippgen et al. 2016). The SRS EFR Network encompasses most major forest types of the southeastern region for long-term studies of southeastern forests. These EFRs have contributed to foundational research on forest management of plantation and natural forests, forestry best management practices (BMPs), catchment hydrological processes, and forest structure and composition dynamics under climate change (Guldin 2009; Loftis 1990; Swank et al. 2001; Swift 1986). The EFRs also serve as important facilities (e.g., eddy covariance flux towers, water chemistry analytic laboratories) for collaborative research, partnerships, and platforms that create cutting-edge science, develop new tools, models, and technologies (Aguilos et al. 2024), and provide research opportunities for a range of other advances, including involvement of women and other underrepresented groups (Laseter et al. 2018; Rustad et al. 2023).

A better understanding of how well the twenty EFRs represent the current southeastern forest conditions will help us to assess how well the southeastern forest will respond to climate change and management. To date, it is unclear how well the SRS EFRs represent southeastern forests in terms of climate, ecosystem structure, and ecosystem functions. Ecosystem structure can be measured by metrics such as leaf area index (LAI) and vegetation height. Ecosystem functions are "the biotic and abiotic processes that occur within an ecosystem and may contribute to ecosystem services either directly or indirectly" (Garland et al. 2021). The southeastern forests are found across variable climate and topographic conditions and are extremely diverse, with differing management regimes (e.g., planted vs natural regeneration). Such climate and management complexity make site synthesis studies that examine the representativeness within the region difficult. Previous studies have assessed how eddy covariance flux sites of the AmeriFlux network represent the US terrestrial ecosystems (Hargrove et al. 2003) and how well sites in the USDA Long-Term Agroecosystems Research (LTAR) Network represent agricultural working lands across the conterminous US (CONUS) (Kumar et al. 2023). In the early 2000s, central continental environments of the CONUS were well represented by AmeriFlux, although additional sites could be needed for south Texas, the Sonoran Desert, and the Pacific Northwest (Hargrove et al. 2003). The LTAR representativeness was good across most of the CONUS (Kumar et al. 2023).

Advances in climate data reanalysis, remote sensing techniques, and cloud-based geospatial computing and mapping platforms (e.g., Google Earth Engine, GEE) over the last two decades now make a variety of data products for measuring climate, ecosystem structure, and ecosystem functions readily available. Gridded climate reanalysis data for the past few decades, such as ERA5-Land (Munoz-Sabater et al. 2021) and MERRA-2 (Gelaro et al. 2017), are available for scales spanning regions to the entire globe. The moderate resolution imaging spectroradiometer (MODIS) sensors on NASA's Earth Observing System (EOS)—Terra and Aqua—provide

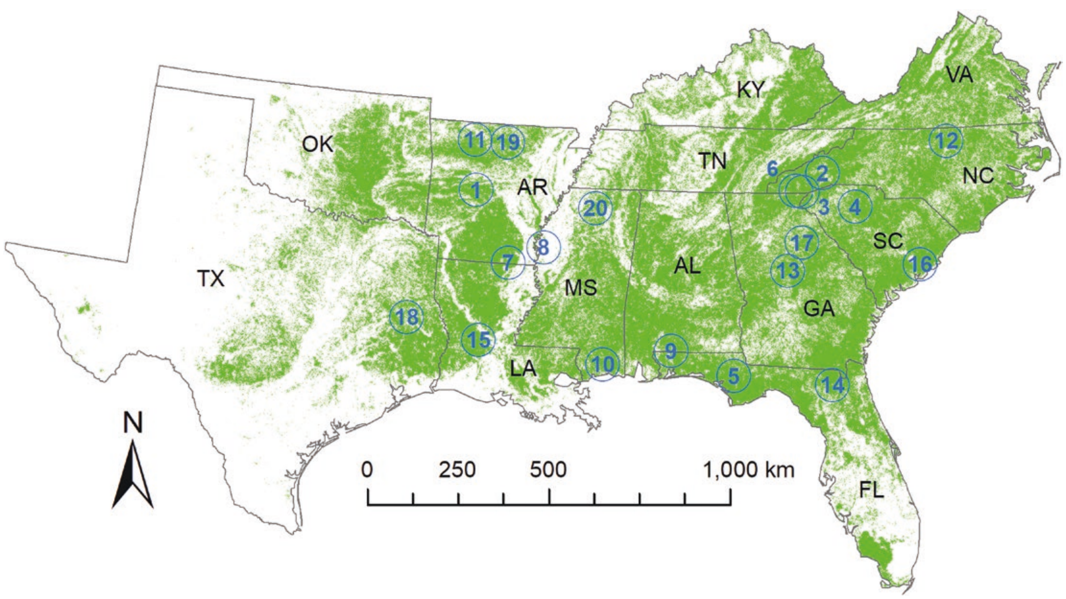

Figure 1 Distribution of southeastern forests and location of the Southern Research Station (SRS) Experimental Forests and Ranges (EFRs). The base map, derived from the National Forest Type dataset (https://data.fs.usda.gov/geodata/rastergateway/forest_type/), shows the distribution of forests across the southeastern forest region. The numbers stand for the EFRs, and the centers of the circles indicate the locations of the EFRs. The numbers are within the circles except for EFRs 3 and 6, as the circles of these two EFRs overlap each other. The names of the EFRs are provided in Table 1.

Table 1. Description of the twenty experimental forests and ranges (EFRs) across the southeastern forest region.

ID	Name	Location	Latitude	Longitude	Area (ha)	Year established
1	Alum Creek Experimental Forest	Central Arkansas	34.79	-93.04	1,885	1959
2	Bent Creek Experimental Forest	Western North Carolina	35.49	-82.63	2,550	1927
3	Blue Valley Experimental Forest	Western North Carolina	35.00	-83.25	526	1964
4	Calhoun Experimental Forest	Northwestern South Carolina	34.62	-81.71	2,078	1947
5	Chipola Experimental Forest	Florida Panhandle	30.43	-85.26	259	1934
6	Coweeta Hydrologic Lab	Western North Carolina	35.06	-83.44	2,218	1934
7	Crossett Experimental Forest	Southeastern Arkansas	33.03	-91.94	680	1934
8	Delta Experimental Forest	Western Mississippi	33.47	-90.90	1,044	1961
9	Escambia Experimental Forest	Southern Alabama	31.01	-87.06	1,214	1947
10	Harrison Experimental Forest	Southern Mississippi	30.63	-89.06	1,662	1934
11	Henry R. Koen Experimental Forest	Northwestern Arkansas	36.04	-93.19	291	1951
12	*Hill Demonstration Forest	North Central North Carolina	36.21	-78.87	1,089	1947
13	Hitchiti Experimental Forest	Central Georgia	33.05	-83.70	1,916	1938
14	Olustee Experimental Forest	Northeastern Florida	30.20	-82.44	1,268	1934
15	Palustris Experimental Forest	Central Louisiana	31.18	-92.67	3,035	1935
16	Santee Experimental Forest	Eastern South Carolina	33.13	-79.81	2,469	1937
17	Scull Shoals Experimental Forest	Central Georgia	33.74	-83.28	1,815	1961
18	Stephen F. Austin Experimental. Forest	Eastern Texas	31.50	-94.77	1,072	1945
19	Sylamore Experimental Forest	Northern Arkansas	36.01	-92.17	1,736	1934
20	Tallahatchie Experimental Forest	Northern Mississippi	34.50	-89.44	1,416	1950

*Cooperating Experimental Forest added to the SRS EFR Network in 2020 based on an agreement between the Forest Service and North Carolina State University.

observations of the Earth's surface, with daily coverage in thirty-six spectral bands and a spatial resolution from 250 m to 1 km for the period from 2000 to the present. The availability of MODIS data along with in situ measurements, data-driven methods, and modeling approaches have led to various data products for quantifying ecosystem structure and functions. For example, MODIS data have been used to develop the global MODIS gross primary production and net primary production (NPP) products in MOD17 (Running et al. 2004), the MODIS evapotranspiration (ET) product in MOD16 (Mu et al. 2011), the MODIS continuous fields (e.g., percentage of tree cover) in MOD44B (DiMiceli et al. 2021), the MODIS LAI in MOD15 (Myneni et al. 2002), and the MODIS aboveground biomass (Blackard et al. 2008). The Global Ecosystem Dynamics Investigation (GEDI), a space-borne LiDAR instrument onboard the International Space Station, provides footprint-based measurements of vegetation structure including forest canopy height between N 52° and S 52° globally (Dubayah et al. 2020). The GEDI observations, along with Landsat data, have been used to develop a global gridded tree-height data product (Potapov et al. 2021).

Here, we used thirteen gridded data products to examine how well the SRS EFRs represent the climate, ecosystem structure, and ecosystem functions of the southeastern forest region. The specific objectives of this study are to (1) assess how the EFRs represent the southeastern forests in terms of the climate using six variables: air temperature, precipitation, shortwave solar radiation, vapor pressure deficit (VPD), soil water content (SW), and drought condition; (2) assess how EFRs represent the southeastern forests in terms of ecosystem functions measured by percentage of tree cover, LAI, and tree height (i.e., tree canopy height); (3) assess how the EFRs represent the southeastern forests in terms of ecosystem functions including NPP, ET, aboveground biomass, and water yield (defined as annual precipitation minus annual ET); (4) use all thirteen variables together to evaluate the representativeness of the SRS EFR network. Representativeness here is defined as how well conditions at sampling locations (i.e., the EFRs) represent conditions across the southeastern region as judged by a combination of the thirteen variables. Our study is unique because it examines the representativeness of the southeastern EFRs in terms of climate, ecosystem structures, and ecosystem functions using several different variables. To the best of our knowledge, this is the first known attempt to evaluate the representativeness of the EFRs using these variables. Assessing how well the EFRs on land that the USDA FS manages represent various forest attributes across the Southeast can help the agency provide research results that are useful for forest managers across ownerships. Our effort can also help researchers and the public understand how well the agency is able to provide that research for the Southeast as well as for the rest of the country.

Materials and Methods

Study Region and EFRs

In this study, the southeastern forest region refers to forests in the thirteen states of the southeastern United States. The twenty EFRs of the SRS EFR Network consist of nineteen official EFRs and one cooperating experimental forest and are distributed across the southeastern region (figure 1; Table 1). Although the nineteen official EFRs possess considerable coverage of forest types, geographical range, and management activities, in 2020, the SRS added a cooperating experimental forest to expand the suite of conditions represented by including studies on university lands (Boggs et al. 2016). Altogether, these EFRs occupy 30,223 ha of land and encompass various landscapes of the region. There is at least one EFR within each of the southeastern states except Kentucky, Oklahoma, Tennessee, and Virginia. The SRS EFRs are located across topographic ranges and environmental gradients and represent a wide range of conditions (e.g., rural to mixed-use landscapes), forest types, and management regimes. We used the National Forest Type dataset from the USDA FS Forest Inventory and Analysis (FIA) program and the Geospatial Technology and Applications Center (GTAC) to assess how the EFRs represented the forest type groups in the region. The forest type groups within each EFR were extracted from this dataset. The twenty EFRs together represent the forest types of the southeastern region well (figure 2). For both the region and the EFRs, the two dominant forest type groups were loblolly/shortleaf pine and oak/hickory; four other types (longleaf/slash pine, oak/pine, oak/gum/cypress, and elm/ash/cottonwood) accounted for >2% of the area each; each of the remaining types accounted for <0.3% of the area.

Climate Data

Climate data were obtained from the widely used ERA5-Land climate reanalysis dataset (Munoz-Sabater et al. 2021) (Table 2). The monthly ERA5-Land data have a spatial resolution of 9 km × 9 km and are available from the GEE. We used monthly average air temperature (Tair), total precipitation (Pre), shortwave solar radiation (SR), dew point temperature, and monthly average volumetric soil water content (SW). Vapor pressure deficit (VPD) was calculated from Tair and dew point temperature at the monthly timescale. VPD was included because it reflects the atmospheric water demand and regulates photosynthesis and transpiration (Li et al. 2023). We then calculated annual mean Tair, annual total Pre, annual mean SR, annual mean VPD, and annual mean SW for 2001 to 2022. Note that these variables (e.g., VPD) were calculated at the annual scale, and deciduous forests might be more sensitive to them over the growing season. We downloaded these gridded data for the southeastern forest region and extracted the time series for each variable for each EFR.

In addition to the climate and SW data, we also used the Palmer Drought Severity Index (PDSI) (Palmer 1965) to estimate drought conditions. The original form of PDSI was used here. Monthly PDSI was derived from the TerraClimate product (Abatzoglou et al. 2018). TerraClimate is a dataset of monthly climate and climatic water balance for global terrestrial surfaces (Abatzoglou et al. 2018) and is also available on the GEE platform. Mean PDSI was calculated for each year from 2001 to 2022 and was downloaded for the southeastern forest region and extracted for each EFR.

Ecosystem Structure Data

We used the following remotely sensed variables to measure ecosystem structure of the EFRs and southeastern forests: percentage of tree cover, LAI, and tree height (Table 2). Other measures of forest structure such as canopy geometry, volume, heterogeneity, and arrangement were not considered as

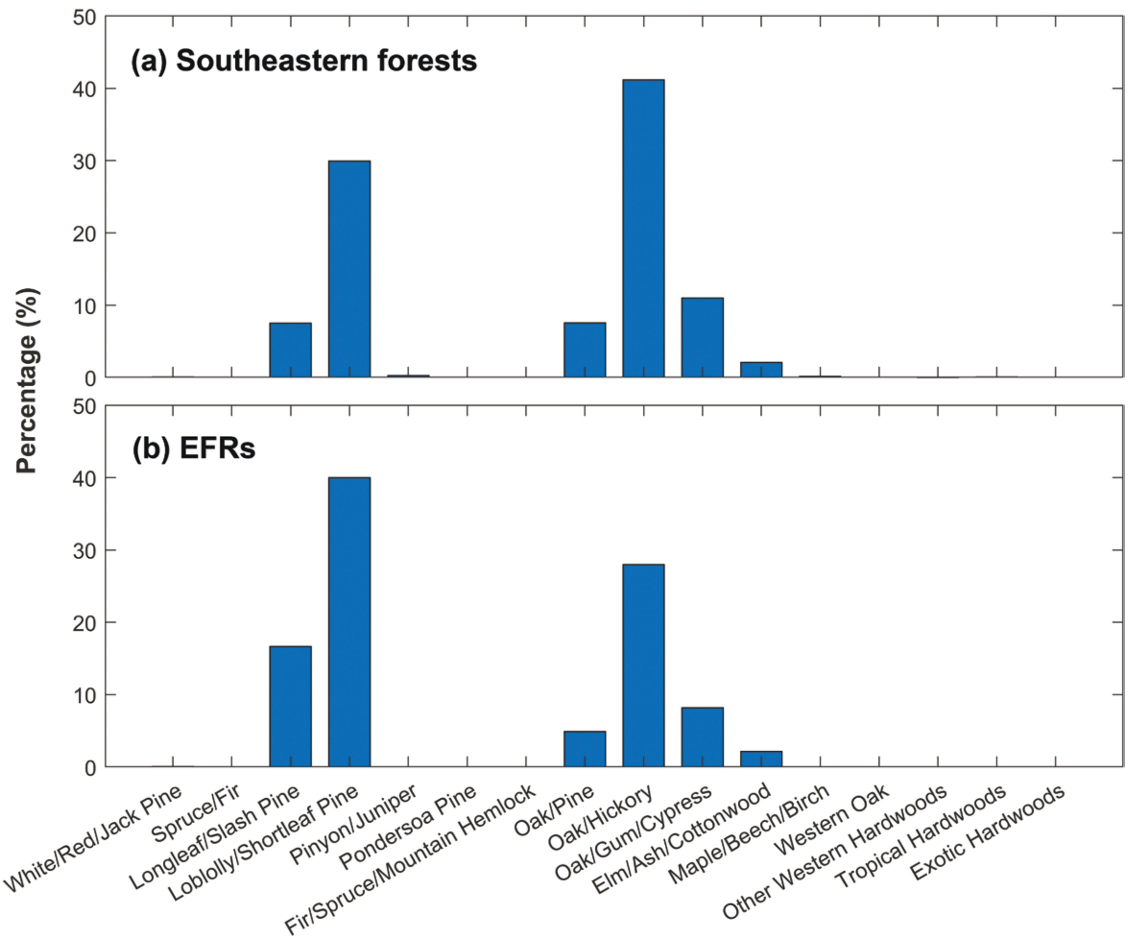

Figure 2 Percentage area of each forest type group for (a) the southeastern region and (b) the EFRs.

Table 2. Summary of the data products used to characterize the climate, ecosystem structure, and ecosystem functions for the southeastern forest region and experimental forests and ranges.

Property	Variable	Data product	Resolution	Duration	Source
Climate	Air temperature (Tair)	ERA5-Land	9 km	2001–2022	Munoz-Sabater et al. 2021
	Precipitation (Pre)	ERA5-Land	9 km	2001–2022	Munoz-Sabater et al. 2021
	Shortwave solar radiation (SR)	ERA5-Land	9 km	2001–2022	Munoz-Sabater et al. 2021
	Soil water content (SW)	ERA5-Land	9 km	2001–2022	Munoz-Sabater et al. 2021
	Vapor pressure deficit (VPD)	ERA5-Land	9 km	2001–2022	Munoz-Sabater et al. 2021
	Palmer Drought Severity Index (PDSI)	TerraClimate	~4 km	2001–2022	Abatzoglou et al. 2018
Ecosystem structure	Percent tree cover	MODIS VCF (MOD44B)	250 m	2001–2020	DiMiceli et al. 2021
	Leaf area index (LAI)	MODIS LAI (MOD15A2)	500 m	2001–2022	Myneni et al. 2002
	Tree height	Global Forest Canopy Height Map	30 m	2019	Potapov et al. 2021
Ecosystem functions	Net primary production (NPP)	MODIS NPP (MOD17A3)	500 m	2001–2022	Running et al. 2004
	Evapotranspiration (ET)	MODIS ET (MOD16A2)	500 m	2001–2022	Mu et al. 2011
	Aboveground biomass (AGB)	FS Forest biomass map	250 m	Circa 2002	Blackard et al. 2008
	Water yield (WY)	ERA5-Land, MODIS ET	500 m*	2001–2022	Munoz-Sabater et al. 2021; Mu et al. 2011

*The resolution of water yield is between 500 and 9 km as it was calculated from the MODIS ET (500 m) and the ERA5-Land (9 km).

gridded data on these measures are not readily available. The percentage of tree cover data were derived from the MODIS Vegetation Continuous Fields (VCF) product of MOD44B (DiMiceli et al. 2021). The VCF product offers a subpixel level representation of vegetation cover globally and consists of estimates of percentage of tree cover, percentage of non-tree cover, and percentage of bare land for each 250 m × 250 m pixel across the global land surface from 2000 to 2020 (DiMiceli et al. 2021). We used the percentage of tree cover data layer to measure tree cover for each EFR and each pixel across the southeastern forest region.

LAI data were obtained from the MODIS Terra LAI product of MOD15A2 (Myneni et al. 2002). The MOD15A2 product provides LAI and fraction of photosynthetically active radiation (FPAR) estimates at the 8-day time step and 500 m × 500 m spatial resolution. LAI, defined as one-half of the total green leaf area per unit ground surface area in broadleaf canopies (Chen and Black 1992) and as the projected needleleaf area in coniferous canopies (Myneni et al. 2002), is a key parameter for depicting vegetation canopy structure and determining the exchange of mass (e.g., carbon dioxide and water) and energy fluxes between the land surface and the atmosphere (Liu et al. 2018). The MOD15A2 product is also available on the GEE platform. Maximum LAI instead of mean (or median) LAI was chosen to measure the ecosystem structure over the peak growing season.

Tree height was based on a new 30 × 30 m spatial resolution global forest canopy height map (Potapov et al. 2021). Here tree height indicates tree canopy height and refers to the vertical distance from the base of a tree to the top of the canopy of the tree. This map was developed for the year 2019 by integrating forest structure measurements from NASA's GEDI instrument and surface reflectance data from NASA's Landsat satellites. This global dataset is also available on the GEE platform. As no high-quality gridded data were available for other years, we were unable to assess the trend in tree height.

Ecosystem Function Data

Besides climate and ecosystem structure data, we also used data on NPP, ET, aboveground biomass (AGB), and water yield (Table 2) to measure ecosystem functions of southeastern forests. Forest water yield and NPP are the critical ecosystem functions that sustain many ecosystem services, such as stable and high-quality water supply, carbon sequestration, climate regulation, and biodiversity conservation (Sun et al. 2011). Estimated annual NPP was based on the MODIS Terra NPP data product (MOD17A3) (Running et al. 2004), which consists of annual NPP estimates at 500 m × 500 m spatial resolution from 2000 to the present. Estimated annual ET was based on the MODIS Terra ET product (MOD16A2) (Mu et al. 2011), an 8-day composite ET product generated at 500 m × 500 m resolution from 2000 to the present. We calculated annual ET from the 8-day ET estimates for 2001 to 2022. Water yield was calculated as the difference between annual precipitation based on the ERA5-Land product and annual ET based on the MODIS ET product from 2001 to 2022. The calculation of water yield was conducted on GEE as both ERA5-Land and MODIS ET are available on the platform.

The AGB data were obtained from the aboveground live forest biomass map with 250 m × 250 m resolution for the conterminous United States, Alaska, and Puerto Rico (Blackard et al. 2008). This map was developed based on plot-level biomass data from the USDA FS FIA program and a variety of spatially continuous data such as MODIS surface reflectance, vegetation indices, and percentage of tree cover, topographic variables, and climate data, along with tree-based regression algorithms (Blackard et al. 2008). This product is also available on the GEE platform.

Analyses

We examined the magnitude and spatial patterns of annual climate variables (i.e., Tair, Pre, SR, VPD, SW, and PDSI) of the southeastern forest region. For each variable, we calculated the long-term mean values from 2001 to 2022 for the region on a per pixel basis and extracted the long-term mean values for each EFR. We then generated the probability density distribution for each variable across the region and assessed to what extent the EFRs represent the region in terms of mean annual climate conditions. In addition, we calculated the long-term trend in each variable for the region from 2001 to 2022 on a per pixel basis using the Mann-Kendall trend test (Kendall 1938; Mann 1945). The Mann-Kendall method is a nonparametric test for monotonic trends, and it does not assume a specific distribution for the data and is insensitive to outliers (Ficklin et al. 2016; Wang et al. 2019). The slopes of the trends were calculated using the Kendall robust line-fit method (Sokal and Rohlf 1995). The time series for each variable was extracted for each EFR, and the long-term trend in each variable was also examined using the Mann-Kendall method.

We then assessed the magnitude and spatial patterns of ecosystem structure as measured by percent tree cover, LAI, and tree height across the region. Percent tree cover and annual maximum LAI were averaged between 2001 and 2022 to calculate long-term mean values on a per pixel basis. The probability density distribution was then generated for each variable. For each EFR, the percentage of tree cover, LAI, and tree height were spatially averaged and extracted. We assessed to what extent EFRs can represent the ecosystem structure of the region. The Mann-Kendall method was used to examine the long-term trend in each variable for the region on a per pixel basis and for each EFR.

Similarly, we assessed the magnitude and spatial patterns of ecosystem functions as measured by NPP, ET, AGB, and water yield for the region. For each variable, the probability density distribution was generated. We calculated the spatially averaged values of long-term means for each variable for each EFR and assessed how the EFRs encompass the ecosystem functions of southeastern forests. We also assessed the long-term trends in ecosystem functions for the region on a per pixel basis and for each EFR.

Finally, we used the thirteen variables in climate (i.e., mean annual Tair, Pre, SR, SW, VPD, PDSI), ecosystem structure (i.e., mean annual percentage of tree cover and LAI and tree height), and ecosystem functions (i.e., mean annual NPP, ET, WY, and AGB) together to assess the representativeness of the SRS EFR network, following Kumar et al. (2023). For this analysis, all the datasets were resampled to the same spatial resolution, whereas for the analyses described above, the native resolution of each dataset was used. Each variable was normalized to the range of [0, 1]. For each EFR or pixel, the values of the thirteen normalized variables were treated as a vector in the multivariate space. To calculate the representativeness of each EFR, we first calculated the Euclidean distance between the vector of the EFR and that of each pixel across the region, and then calculated the representativeness of each EFR as follows:

$$representativeness = 1 - \sqrt{\sum_{i=1}^{13} \left(V_i^{EFR} - V_i^{pixel} \right)^2} \quad (1)$$

where V_i^{EFR} and V_i^{pixel} stand for the multivariate vector for the EFR and a given pixel, respectively. For each EFR, we generated a representativeness map for the region, in which a higher value indicates that the pixel is closer to the EFR in the multivariate space and that the EFR is more representative of that pixel. To assess the representativeness of the SRS EFR network, we calculated the maximum representativeness value among the values of the 20 EFRs for each pixel.

Results

Climate

We first examined the long-term means of annual mean temperature, annual precipitation, annual mean shortwave solar radiation, annual mean VPD, annual mean soil water content, and PDSI for the southeastern forest region (figure 3) and the EFRs (Figure S1) between 2001 and 2022. We also compared the long-term means of these variables for the EFRs against the probability density distribution of these variables for the entire southeastern forest region (figure 4). Tair generally increased with decreasing latitude, except in the Appalachian Mountains (figure 3a). Tair ranged from ~9°C to 25°C across the region (figure 4a). The twenty EFRs encompassed a large portion of the distribution of Tair across the region, whereas areas with Tair above 20.6°C or below 12.0°C (mostly in the tails of the probability distribution) had no EFR representation (figure 4a). Unlike Tair, Pre showed intermediate values in the states on the East Coast (Virginia, North Carolina, South Carolina, Georgia, Florida), low values in the West (Oklahoma and Texas), and high values in the central parts of the region (figure 3b). The annual Pre across the region ranged from ~500 to ~1700 mm yr^{-1}, whereas the Pre of the EFRs was between 1074 and 1518 mm yr^{-1}; a significant portion of the region (the majority of Oklahoma and Texas and a small part of the states on the East Coast) had Pre < 1000 mm yr^{-1} and had no EFR representation (figures 3b and 4b). SR had a similar spatial pattern to Tair (figure 3a and c), and areas with SR lower than 182 W m^{-2} or higher than 197 W m^{-2} contained no EFRs (figure 4c). The differences in solar radiation are largely caused by the changes in sun elevation angle that varies with latitude and changes in cloud over. The spatial pattern of VPD was similar to that of Tair or SR (figure 3). The VPD of the twenty EFRs centered around the peak value of the probability density distribution of the region and ranged from 4.0 to 8.2 hPa; two EFRs had VPD < 4.0 hPa, whereas no EFR had VPD > 8.2 hPa (figure 4d). SW had relatively low values in the southeast of the region (e.g., Georgia, Florida) (figure 3e); the EFRs altogether encompassed the distribution of SW well (figure 4e). The long-term mean PDSI map indicates that the northern and central parts of the region were relatively wet whereas the western, southern, and eastern parts of the region were relatively dry (figure 3f); the PDSI value of the twenty EFRs ranged from -0.6 to 0.7, covering a large portion of the distribution of PDSI over the southeastern forest region (figure 4f).

The trends in Tair, SR, VPD, and SW varied substantially across the southeastern forest region (figure 5). The southeastern half of the region had increasing trends in Tair, whereas the rest of the region except Texas had decreasing trends in Tair (figure 5a); the trends in Tair were statistically significant for only a small portion of the region (Figure S2). Among the twenty EFRs, only one EFR (Harrison, in southern Mississippi) had a statistically significant trend in Tair (Figure S3). SR exhibited an increasing trend in the Appalachian Mountains and areas in Oklahoma and Texas but a declining trend in the rest of the region (figure 5c). None of the EFRs had a statistically significant trend in SR (Figure S3). Compared with Tair, SR, and SW, Pre, VPD, and PDSI were more spatially consistent in the direction of change across

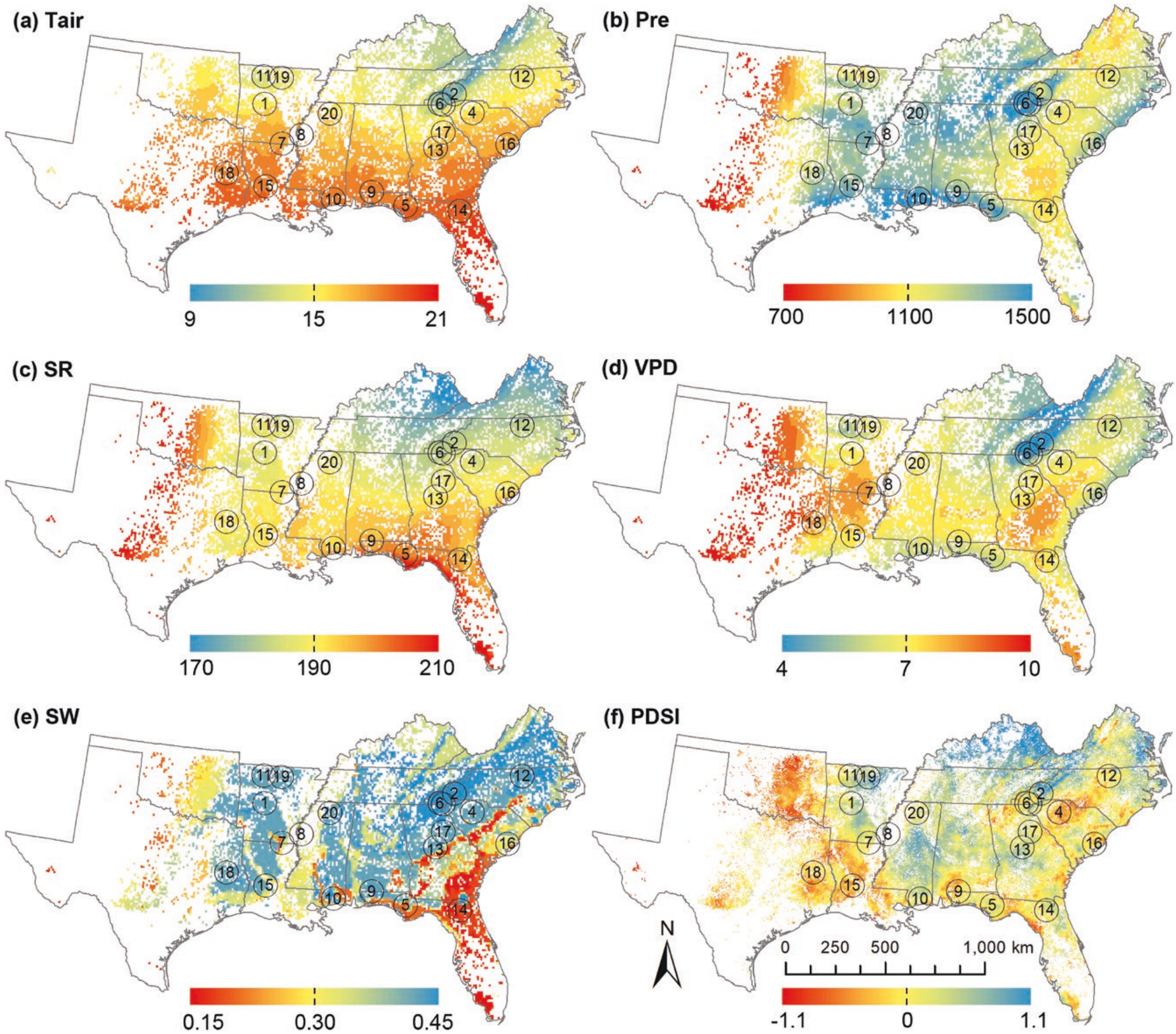

Figure 3 Magnitude and spatial pattern of mean annual (a) temperature (Tair; °C), (b) precipitation (Pre; mm), (c) shortwave solar radiation (SR; W m^{-2}), (d) vapor pressure deficit (VPD; hPa), (e) volumetric soil water content (SW; unitless), and (f) PDSI from 2001 to 2022 for the southeastern forest region. The numbers in circles stand for experimental forests and ranges (EFRs); the correspondence between the numbers and the EFRs is provided in Table 1.

the region. Most of the region had upward trends in VPD, and only areas in Louisiana and southern Florida exhibited downward trends (figure 5d). The VPD trend was statistically insignificant for all the EFRs (Figure S3). The entire region except a small area in Texas exhibited an increasing trend in Pre and PDSI (figure 5b, f). The trend in Pre was statistically significant for three EFRs (Henry R. Koen in northwestern Arkansas, Palustris in central Louisiana, and Santee in eastern South Carolina). None of the EFRs had a significant trend in VPD. The PDSI trend was significant for five EFRs: Alum Creek (central Arkansas), Bent Creek (western North Carolina), Chipola (Florida panhandle), Harrison, and Olustee (northeastern Florida) (Figure S3).

Ecosystem Structure

We examined the ecosystem structure indicators of the southeastern forest region (figure 6) and EFRs (Figure S4) based on percentage of tree cover, maximum LAI, and tree height. Percentage of tree cover exhibited the highest values (>80%) in the Appalachian Mountains, the lowest values in Oklahoma, Texas, and sporadic areas in the states of the East Coast (figure 6a). The probability density distribution of percentage of tree cover across the region showed that percentage of tree cover primarily ranged from 0% to 80% and peaked around 50%; the percentage of tree cover of the EFRs ranged from 46% (Delta in western Mississippi) to 72% (Coweeta Hydrologic Laboratory in western North Carolina) (figure 7a). Compared with percentage of tree cover, LAI was more homogenous across southeastern forests. Most of the region had high LAI values, whereas areas within Oklahoma and Texas had low values; the remaining areas had intermediate values (figure 6b). The distribution of LAI across the region peaked at ~6.7; the LAI of the twenty EFRs ranged from 5.1 (Escambia in southern Alabama) to 6.8 (Coweeta Hydrologic Laboratory); there were no EFRs in areas with LAI lower than 5 (figure 7b). Tree height had high values in

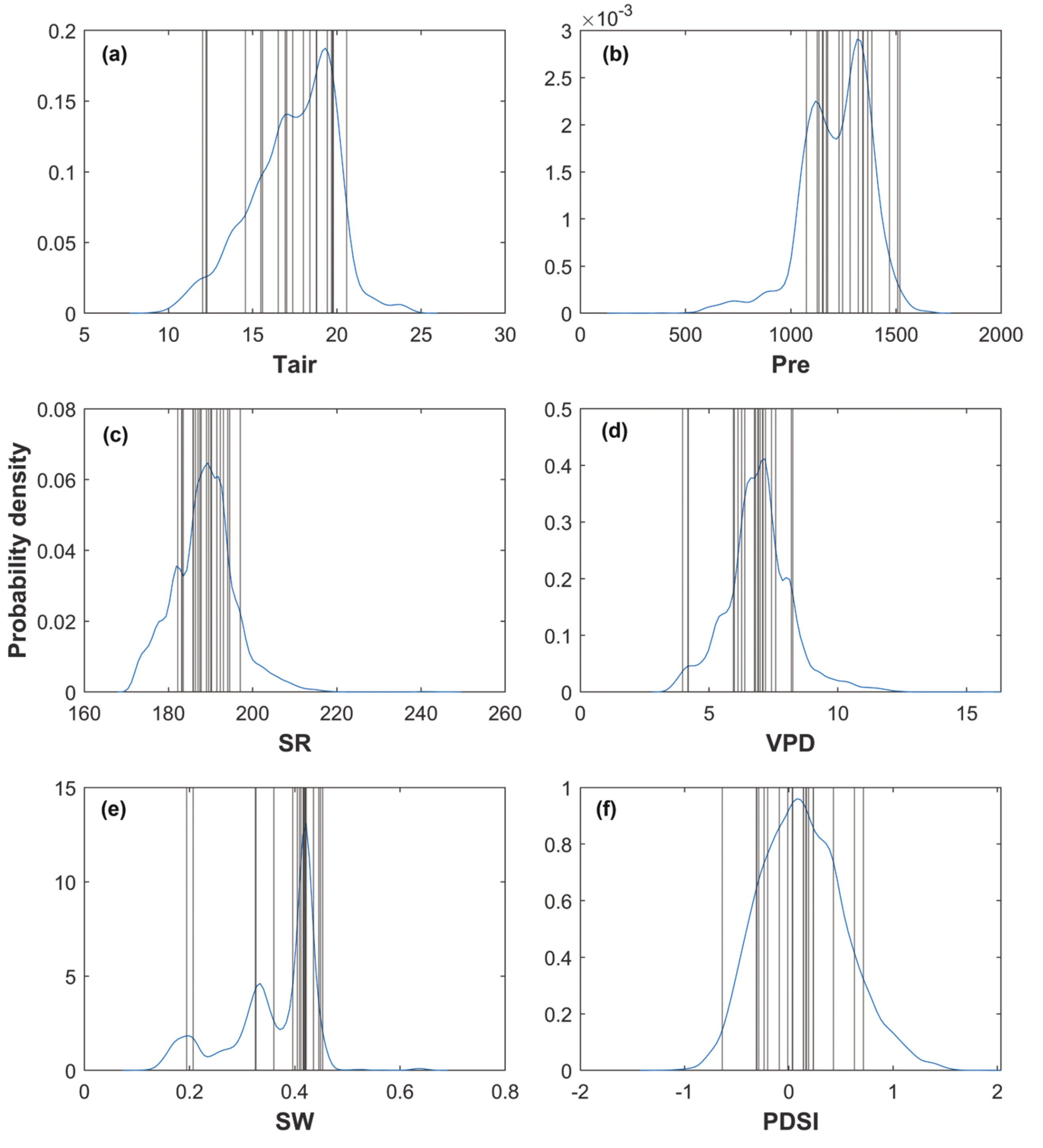

Figure 4 Probability density distribution of mean annual (a) temperature (Tair; °C), (b) precipitation (Pre; mm yr^{-1}), (c) shortwave solar radiation (SR; W m^{-2}), (d) vapor pressure deficit (VPD; hPa), (e) volumetric soil water content (SW; unitless), and (f) PDSI from 2001 to 2022 across the southeastern forest region. The vertical lines indicate the mean annual values for the EFRs.

the Appalachian Mountains, low values in areas in Oklahoma and Texas as well as sporadic areas in the states on the East Coast, and intermediate values in the rest of the southeastern forest region (figure 6c). The probability density distribution of tree height peaked at ~20m. The tree height of the majority of the EFRs ranged from 17 to 24 m; Alum Creek and Bent Creek had an average tree height of 8 and 11 m, respectively, whereas Sylamore in northern Arkansas and Tallahatchie in northern Mississippi had an average tree height of 27 and 28 m, respectively (figure 7c).

We then examined the long-term trends in percentage of tree cover and maximum LAI (figure 8). The trends were statistically significant for a large fraction of the pixels (Figure S5). No widespread areas exhibited either upward or downward trends in percentage of tree cover; instead, pixels with upward trends in percentage of tree cover were interspersed with those with

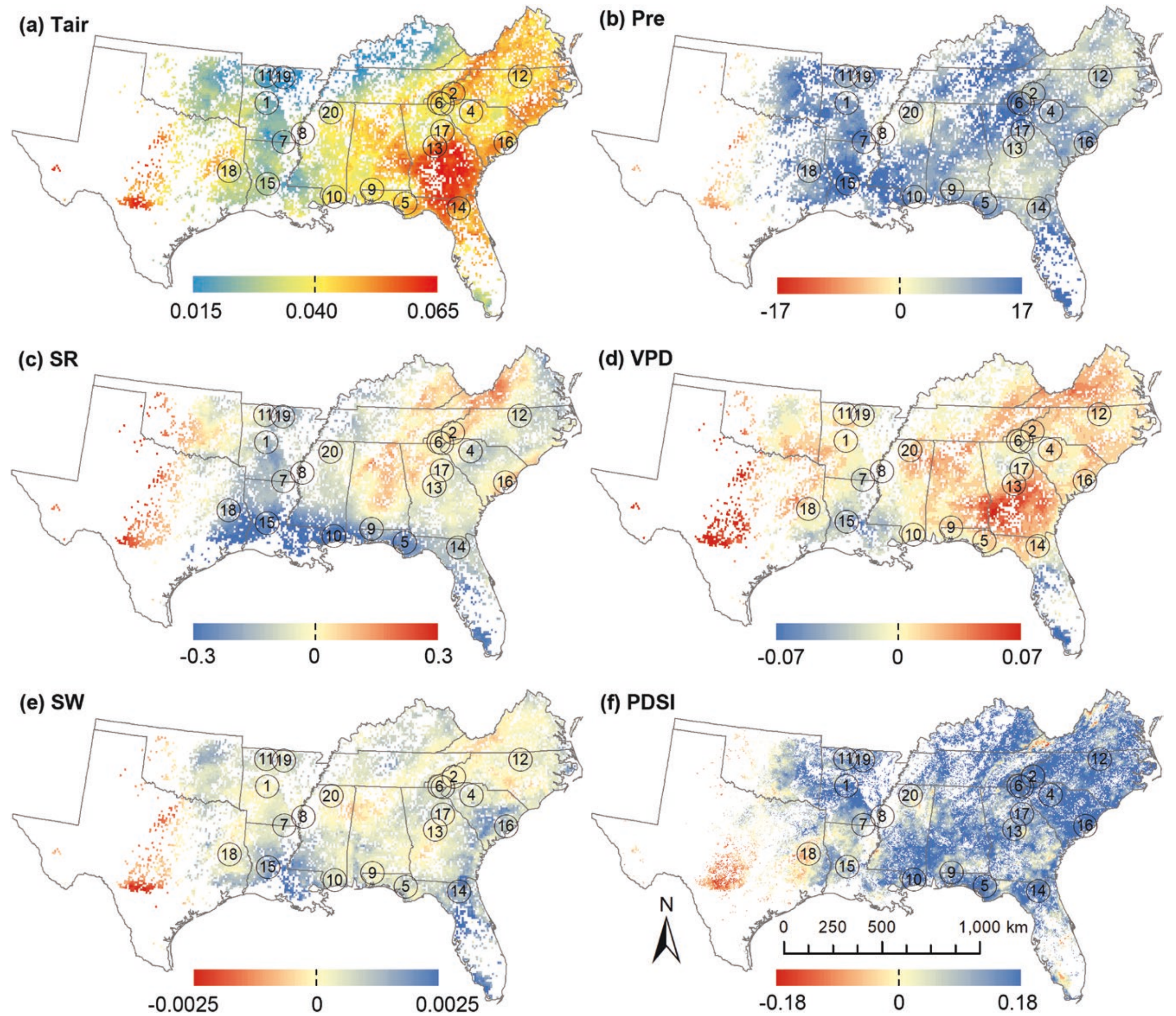

Figure 5 Long-term trends of annual (a) temperature (Tair; °C yr⁻¹), (b) precipitation (Pre; mm yr⁻¹), (c) shortwave solar radiation (SR; W m⁻² yr⁻¹), (d) vapor pressure deficit (VPD; hPa yr⁻¹), (e) volumetric soil water content (SW; % yr⁻¹), and (f) PDSI from 2001 to 2022 for the southeastern forest region. The numbers in circles stand for experimental forests and ranges (EFRs); the correspondence between the numbers and the EFRs is provided in Table 1.

downward percentage of tree cover (figure 8a). Seven EFRs had upward trends in percentage of tree cover, but none of the trends were statistically significant; the remaining thirteen EFRs had downward trends, and four of them (Bent Creek, Chipola, Sylamore, and Tallahatchie) had statistically significant trends ($p < .05$) (Figure S6). Many areas of the region (e.g., western North Carolina, South Carolina, Georgia, Alabama, southern Mississippi, and Oklahoma) had increasing trends in LAI, whereas the Appalachian Mountains and some other areas of the region had nearly no trends in LAI (figure 8b). The spatially averaged LAI had an increasing trend for all the EFRs except Chipola, Santee, and Tallahatchie, and the increasing trend was statistically significant for seven EFRs (Figure S6). We were not able to explore the long-term trend in tree height as the tree height map is only available for 2019.

Ecosystem Functions

Along with climate and ecosystem structure, we also examined the ecosystem functions in ecosystem productivity and water cycle regulation in the southeastern forests (figure 9) and EFRs (Figure S7) using four indicators: mean annual NPP, ET, water yield, and AGB. All these metrics exhibited relatively large variability across the southeastern forest region (figure 9). Annual NPP had the highest values in the Appalachian Mountains, western Louisiana/eastern Texas, southern Mississippi, Florida, and coastal areas of Georgia and the Carolinas, the lowest values in central and southern Arkansas, northern Louisiana, and northern Mississippi, and intermediate values in other areas of the region (figure 9a). The mean annual NPP of the twenty EFRs had a large range, varying from 257 g C m^{-2} yr^{-1} (Crossett in southeastern Arkansas) to 1145 g C m^{-2} yr^{-1} (Harrison) (Figure S7) and well encompassed the distribution of the NPP of the region (figure 10a). Mean annual ET generally increased with decreasing latitude across the region, except in the Appalachian Mountains and Texas (figure 9b). A large portion of the southeastern forest region had annual ET between 500 and 900 mm yr^{-1}, and the ET of 18 EFRs was within this range

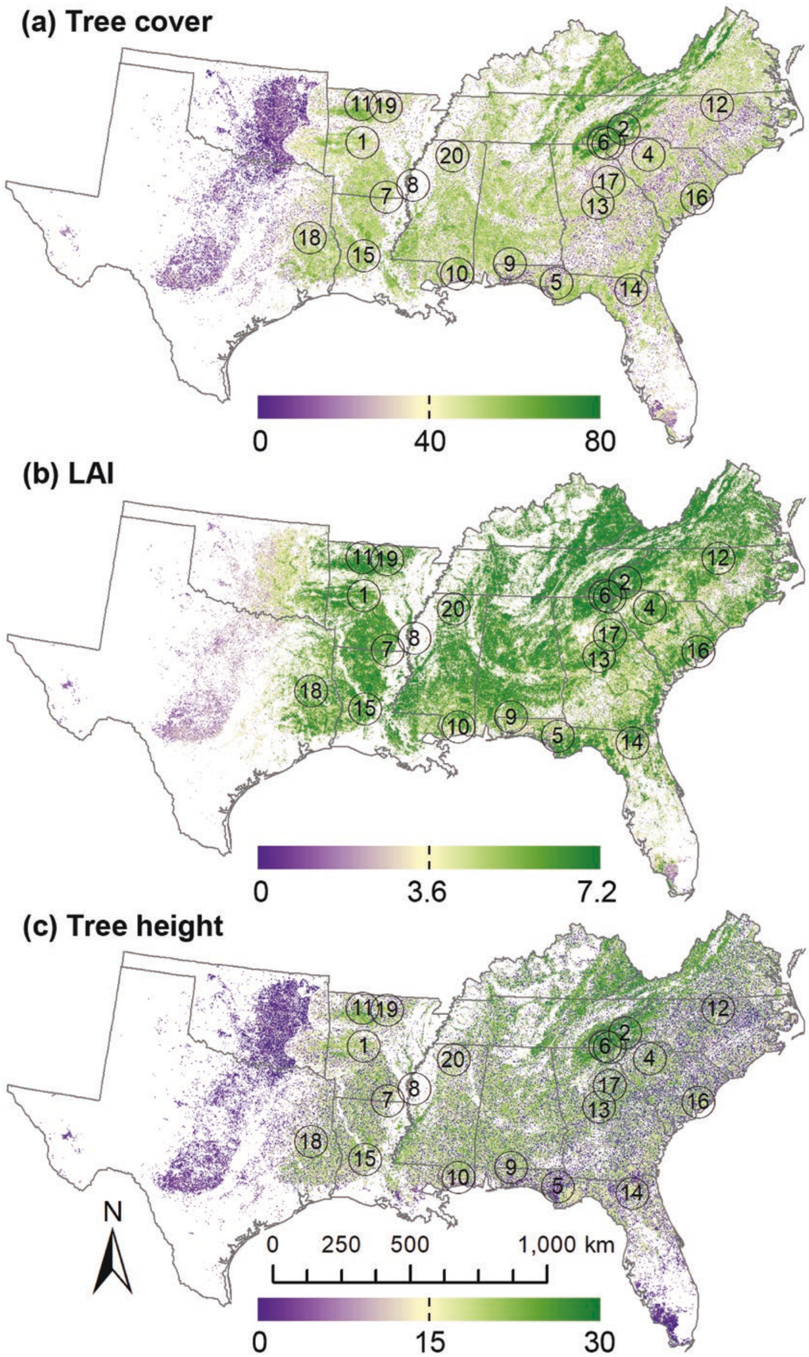

Figure 6 Magnitude and spatial pattern of (a) long-term mean percentage of tree cover (%) (2001 to 2020), (b) long-term mean of maximum leaf area index (LAI) (2001 to 2022), and (c) tree height (2019) for the southeastern forest region. The numbers in circles stand for experimental forests and ranges (EFRs); the correspondence between the numbers and the EFRs is provided in Table 1.

(figure 10b); Coweeta Hydrologic Laboratory and Olustee had the lowest (432 mm yr^{-1}) and highest ET (934 mm yr^{-1}), respectively (Figure S7). The AGB was highest in North Carolina and northern Virginia, intermediate in southern Virginia, Kentucky, Tennessee, Arkansas, Mississippi, northern Georgia, and Florida, and the lowest in other areas of the region (figure 9c). The probability density distribution of AGB across the region peaked at ~100 Mg ha^{-1}. The AGB of sixteen EFRs centered around the peak value of the distribution (i.e., mode) and ranged from 81 to 127 Mg ha^{-1}, whereas the remaining four EFRs had much higher AGB: Coweeta Hydrologic Laboratory (164 Mg ha^{-1}), Hill Demonstration Forest in central North Carolina (171.7 Mg/ha), Bent Creek (187 Mg ha^{-1}), and Blue Valley in western North Carolina (202 Mg ha^{-1}) (figure 10c; Figure S7). The annual water yield had high values in the Appalachian Mountains and Arkansas; intermediate values in eastern Virginia, eastern portions of North Carolina, northern South Carolina, Louisiana, southern Mississippi, and central Alabama; and low values in western Virginia, western North Carolina, Georgia, northern Florida, southern Alabama, Oklahoma, and Texas (figure 9d). Notably, Olustee Experimental Forest had low water yield

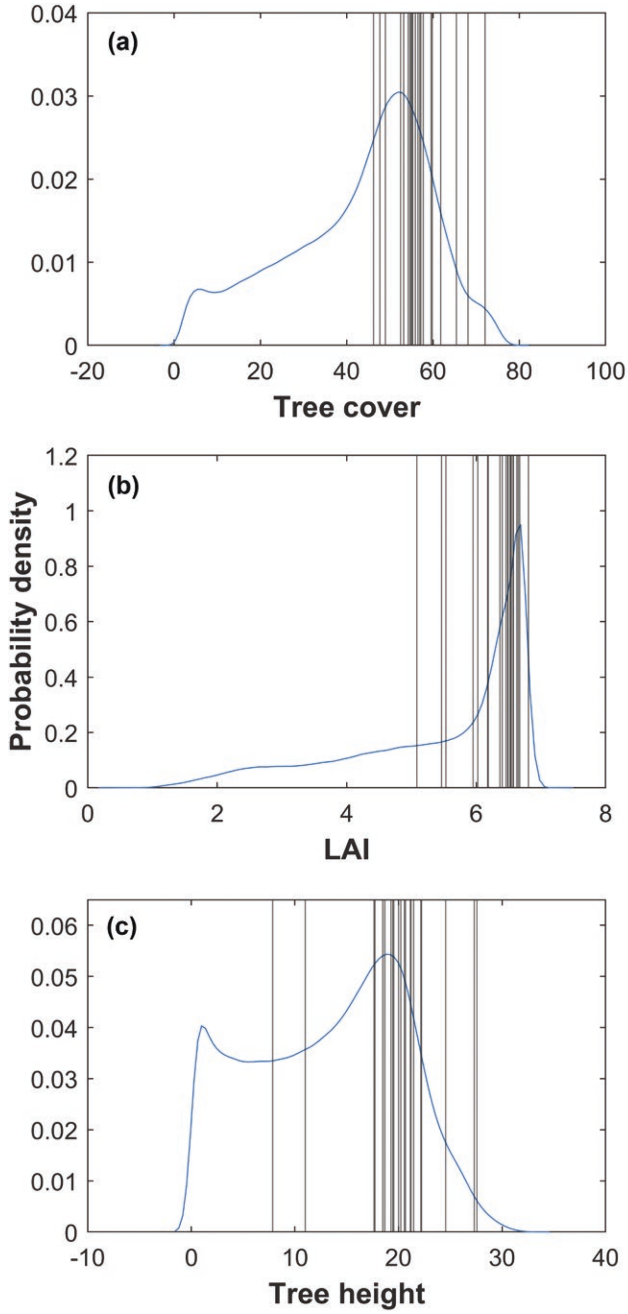

Figure 7 Probability density distribution of (a) long-term mean annual tree cover (%) (2001 to 2020), (b) long-term mean of maximum leaf area index (LAI) (2001 to 2022), and (c) tree height (m) across the southeastern forest region. The vertical lines indicate the average values for the twenty experimental forests and ranges.

but high NPP (Figure S7a and d). The probability density distribution of annual water yield of the southeastern forest region peaked at ~250 mm yr^{-1}; only one EFR (Olustee) had water yield lower than this value (figure 10d). Among the remaining nineteen EFRs, four EFRs (Crossett: 609 mm yr^{-1}; Coweeta Hydrologic Laboratory: 675 mm yr^{-1}; Blue Valley: 707 mm yr^{-1}; Delta: 733 mm yr^{-1}) had water yield greater than 600 mm yr^{-1}; the water yield of the other fifteen EFRs ranged from 283 to 526 mm yr^{-1} (Figure S7).

We then assessed the long-term trends in annual NPP, ET, and water yield over the period 2001–2022 for the southeastern forest region on a per pixel basis (figure 11; Figure S8) and for each EFR (Figure S9). The NPP exhibited increasing trends in the entire region except in some areas (e.g., areas along the East Coast and Gulf Coast, and a part of Texas) (figure 11a); eighteen EFRs had increasing trends in NPP but only two of them (Hill Demonstration Forest and Tallahatchie) had statistically significant trends ($p < .05$); Chipola and Henry R. Koen (in northwest Arkansas) had insignificant decreasing trends ($p > .05$) (Figure S9). Increasing trends in annual ET were observed for nearly the entire southeastern forest region (figure 11b); eighteen EFRs had increasing trends in ET, and the trend was significant for eleven of these EFRs; two EFRs (Chipola and Coweeta Hydrologic Laboratory) had insignificant decreasing trends in ET (Figure S9). Unlike NPP and ET, water yield exhibited large variability in the direction of change across the region; an increasing trend in water yield was found in the Appalachian Mountains, northern Arkansas, northeastern Oklahoma, Louisiana, southern Mississippi, and parts of Florida and South Carolina (figure 11c); twelve and eight EFRs had upward and downward trends in water yield, respectively, whereas none of the trends were statistically significant (Figure S9). The long-term trend in AGB was not examined because the gridded AGB data were not available yearly for a long period of time.

Representativeness Based on all Thirteen Variables

The representativeness of specific EFRs varies substantially among the EFRs (figure 12). Some EFRs only represent a very small part of the region well but others are well representative of a significant portion of the region. For example, two EFRs (Calhoun Experimental Forest, #4; Coweeta Hydrologic Laboratory, #6) are only representative of the Appalachian Mountains area adjoining North Carolina, South Carolina, Georgia, and Tennessee, and the Chipola Experimental Forest (#5) is only well representative of the Florida Panhandle. By contrast, some EFRs such as Alum Creek (#1), Hitchiti (#13), Scull Shoals (#17), and Tallahatchie (#20) are representative of a sizable portion of the southeastern region. The SRS EFR network overall, however, represents a large portion of the region relatively well, whereas central Oklahoma and Texas are least represented (figure 13).

Discussion

We used a variety of gridded datasets to assess how the twenty EFRs represent the southeastern forests. The southeastern forest region is dominated by a humid, subtropical climate that is influenced by various factors such as latitude, topography, and proximity to the Gulf of Mexico and Atlantic Ocean (Carter et al. 2018). The southeastern forest region has relatively large gradients in mean annual climate (i.e., Tair, Pre, SR, VPD), SW, and PDSI. Temperature generally decreases with increasing latitude and elevation (Carter et al. 2018). Altogether, the twenty EFRs encompass a large range of the distribution of each climate variable, whereas the areas with low and high values (often in the tails of the probability distributions) are typically underrepresented or have no EFRs at all. Understanding the tails of the climate distributions is important as ecosystems in these areas are likely more sensitive to climate change. For example, dryland ecosystems are more sensitive to changes in precipitation, whereas ecosystems in areas with high temperatures are more susceptible to warmer temperatures. To improve the representativeness of

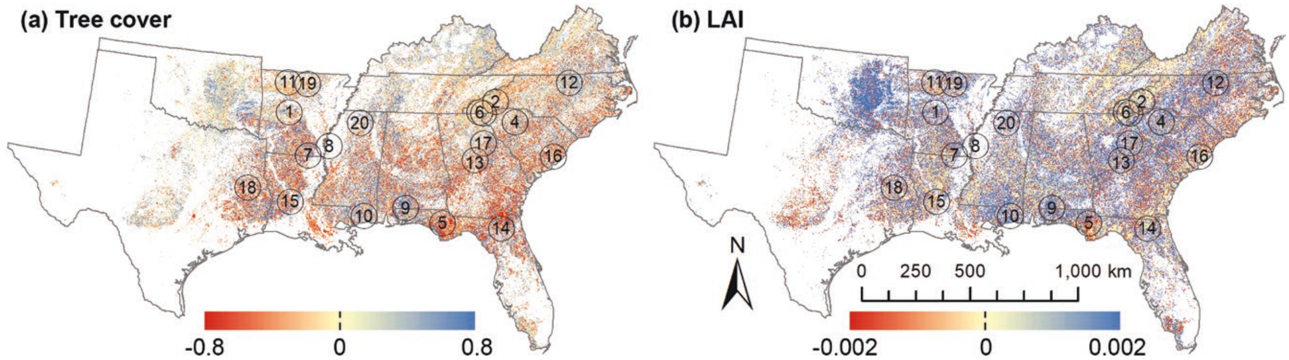

Figure 8 Long-term trends of (a) percentage of tree cover (% yr^{-1}) and (b) maximum leaf area index (LAI) for southeastern forests from 2001 to 2020 and from 2001 to 2022, respectively. The numbers in circles stand for experimental forests and ranges (EFRs); the correspondence between the numbers and the EFRs is provided in Table 1.

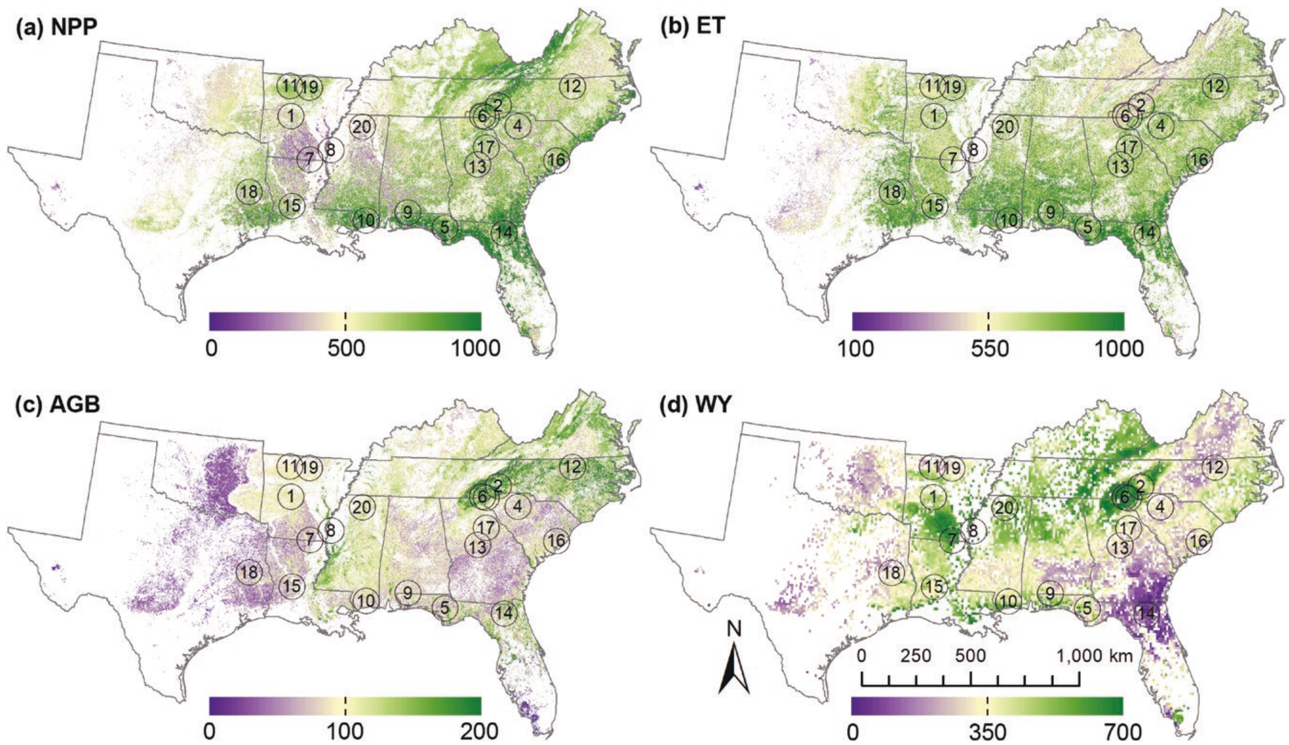

Figure 9 Magnitude and spatial pattern of (a) mean annual net primary production (NPP; g C m^{-2} yr^{-1}) (2001 to 2022), (b) mean annual evapotranspiration (ET; mm yr^{-1}) (2001 to 2022), (c) aboveground biomass (AGB; Mg ha^{-1}), and (d) mean annual water yield (WY; mm yr^{-1}) (2001 to 2022) for the southeastern forest region. The numbers in circles stand for experimental forests and ranges (EFRs); and the correspondence between the numbers and the EFRs is provided in Table 1.

the mean climate conditions across the southeastern forest region, additional EFRs could be established in areas such as the Appalachian Mountains of Virginia, southern Florida, Oklahoma, and central/northern Texas. A large portion of the forests across the southeastern forest region has intermediate to higher percentage of tree cover and LAI, and a sizable portion of the region has relatively low tree height. All the EFRs have intermediate and high values in ecosystem structure metrics (i.e., percentage of tree cover, LAI, and tree height). Establishing EFRs in forests with relatively low percentage of tree cover, LAI, or tree height or in young forests could improve the representativeness of EFRs in terms of ecosystem structure, as none of the EFRs has a percentage of tree cover lower than 45%, maximum LAI lower than 4.5, or tree height lower than 7.9 m. The lack of representation for areas with low tree cover, LAI, and/or tree height is perhaps not surprising because all of the EFRs in the southeastern region are experimental forests (not experimental ranges), but additions to the network could also include experimental ranges that focus on grassland and savanna systems, such as the Cross Timbers region of eastern Oklahoma and north-central Texas (Hallgren et al. 2012). Ecosystem functions as measured by NPP, ET, AGB, and water yield exhibited large gradients across the southeastern forest region. A large portion of the distribution for both NPP and ET is well represented by the EFRs. Establishing EFRs in areas with intermediate and low AGB and water yield, such as large parts of South Carolina, Georgia, Oklahoma, and Texas, could improve the representativeness of the EFRs in terms of AGB and water yield. These areas have intermediate or low biomass because

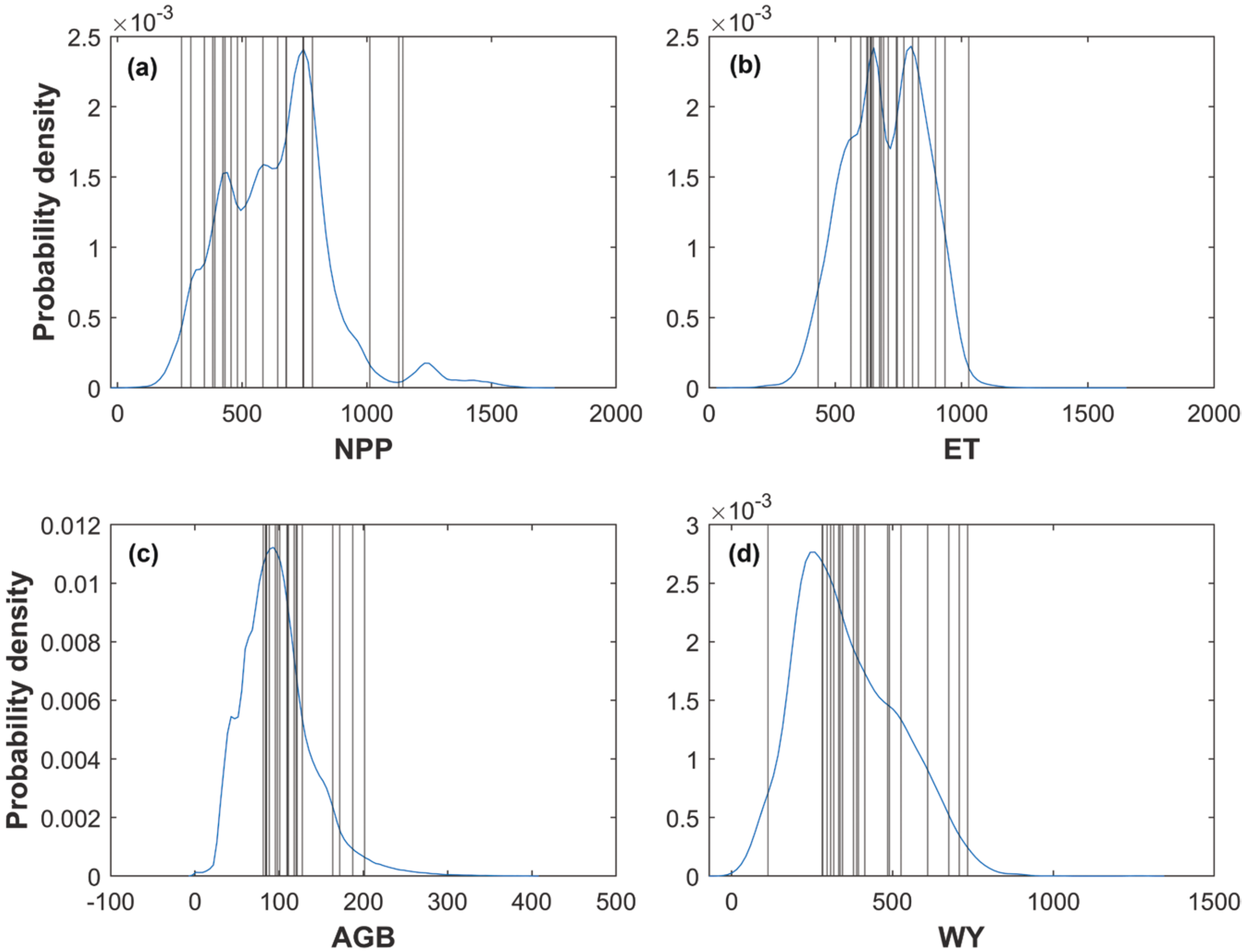

Figure 10 Probability density distribution of (a) mean annual net primary production (NPP; g C m^{-2} yr^{-1}) (2001 to 2022), (b) mean annual evapotranspiration (ET; mm yr^{-1}) (2001 to 2022), (c) aboveground biomass (AGB; Mg ha^{-1}), and (d) mean annual water yield (WY; mm yr^{-1}) (2001 to 2022) across the southeastern forest region. The vertical lines indicate the average values for the experimental forests and ranges.

of intermediate or low annual precipitation, tree height, and LAI and have intermediate or low water yield because of intermediate or low precipitation but intermediate or high temperature and/or VPD.

The long-term trends in the climate-related variables (i.e., Tair, Pre, SR, VPD, SW, and PDSI) were generally consistent between the EFRs and the southeastern forest region. For example, Tair had an increasing trend for nearly every location across the region, and all the EFRs had increasing trends in Tair; SR exhibited negative trends for nearly the entire southeastern forest region, and the majority of the EFRs (sixteen of twenty) also had negative trends in SR. This indicates that these EFRs are generally representative of the region in terms of climate trends. The trends in percentage of tree cover and LAI were also generally consistent between the region and the EFRs. On a per pixel basis, increases and decreases in percentage tree cover were interspersed with each other, and seven and thirteen EFRs had increasing and decreasing percentage of tree cover, respectively; increasing LAI was observed for most of the pixels in the region and seventeen of the twenty EFRs. The trends in ecosystem functions (i.e., NPP, ET, and water yield) of the EFRs were also generally representative of those of the region.

Ecosystem structure and functions could exhibit spatial variability within a given EFR. For example, although on average, none of the EFRs have low percentage of tree cover or tree height or young forests, short or young trees could exist in any given EFR. Assessing the variability within each EFR is limited by the spatial resolution of the data used. The smallest EFR has an area of 259 ha (~2.6 km^2), whereas the spatial resolution (or grid cell size) of most of the datasets ranges from 500 m to 4 km. The only dataset that is suitable for assessing within-EFR variability is the tree height dataset that is at 30 m resolution. We used this dataset to assess whether the distribution of tree height for these 30 m grid cells could better represent that of the southeastern forests (Figure S10). With all the 30 m grid cells within each EFR considered, the tree height of the EFRs mainly ranges from 18 to 24 m, and still underrepresents medium and relatively short trees.

It should be noted that there are other research forests across the southeastern region other than the EFRs. Notably, there are other research forests on federal or state lands. Moreover, some universities have their own research forests. For example, the Duke Forest in North Carolina, which is owned and managed by Duke University, consists of more than 2,800 ha of forested land and has been managed for research experiments

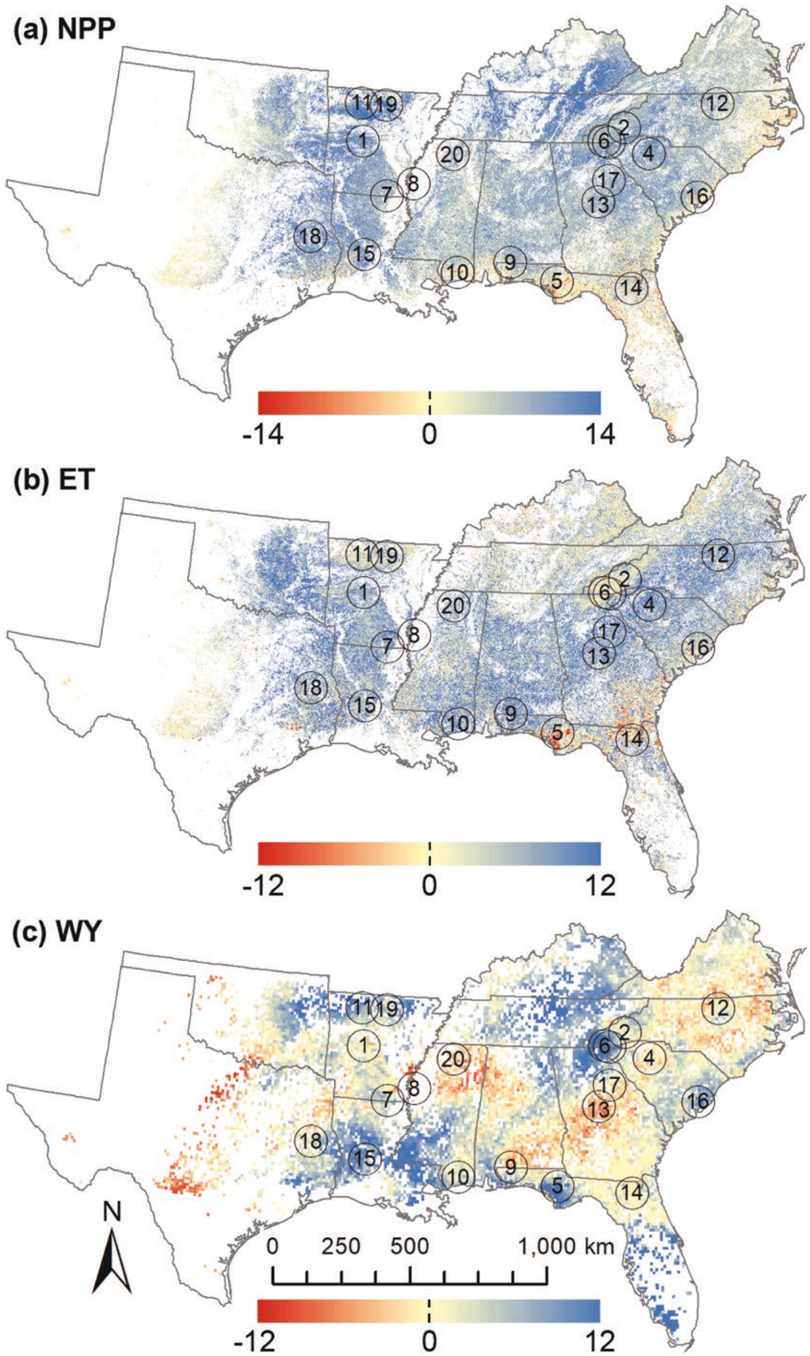

Figure 11 Trends of annual (a) net primary production (NPP; g C m^{-2} yr^{-1}), (b) evapotranspiration (ET; mm yr^{-1}), and (c) water yield (WY; mm yr^{-1}) for the southeastern forest region from 2001 to 2022. The numbers in circles stand for experimental forests and ranges (EFRs); the correspondence between the numbers and the EFRs is provided in Table 1.

(e.g., free-air carbon dioxide enrichment or FACE). Although these forests are not part of the EFR network, tremendous research has been done to examine ecosystem functions and services amidst climate change based on these sites. These research forests, in combination with the EFRs, are likely able to better represent the southeastern forests in terms of climate, ecosystem functions, and ecosystem structure than the EFR network alone and to better answer science questions related to climate change, disturbance, and management practices.

Future representativeness studies of the EFRs could benefit in the following ways. First, using climate and PDSI data with finer spatial resolution can better characterize climate and drought conditions of the EFRs, particularly the small ones. Second, besides the magnitude and trends in annual climate variables, the seasonality of climate could be considered. Third, the future availability of time series data for AGB and tree height will allow for the characterization of the temporal dynamics of these two variables. Finally, besides climate, ecosystem functions, and ecosystem services, other aspects, such as soil properties, elevation, stand age, and structural diversity (Crockett et al. 2023) could be incorporated into future representativeness assessments.

This study across the EFRs and the southeastern forest region fills the knowledge gap regarding the climate, ecosystem

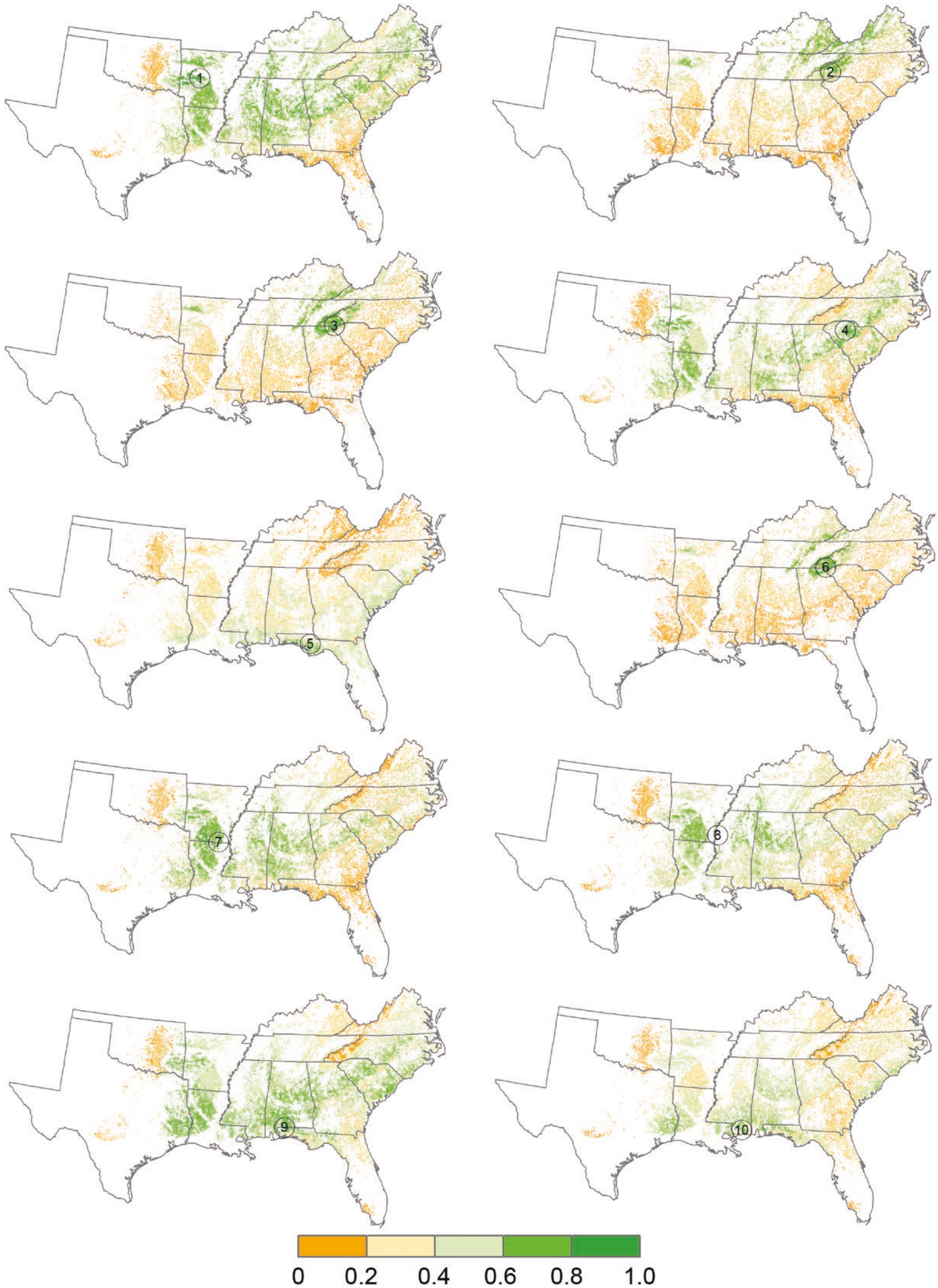

Figure 12 Representativeness of each EFR based on the thirteen variables in climate, ecosystem structure, and ecosystem functions together. The representativeness was calculated based on Equation 1. The numbers in circles stand for EFRs; the names of the EFRs are provided in Table 1.

structure, and ecosystem functions of EFRs in the context of the broader southeastern forest region. Understanding ecosystem functions and structures across the EFR network can help the SRS to address new research questions, including those associated with expected climate change across the southeastern forest region during the remainder of the twenty-first century (Carter et al. 2018). Although projected increases in temperature for some parts of the region are smaller than

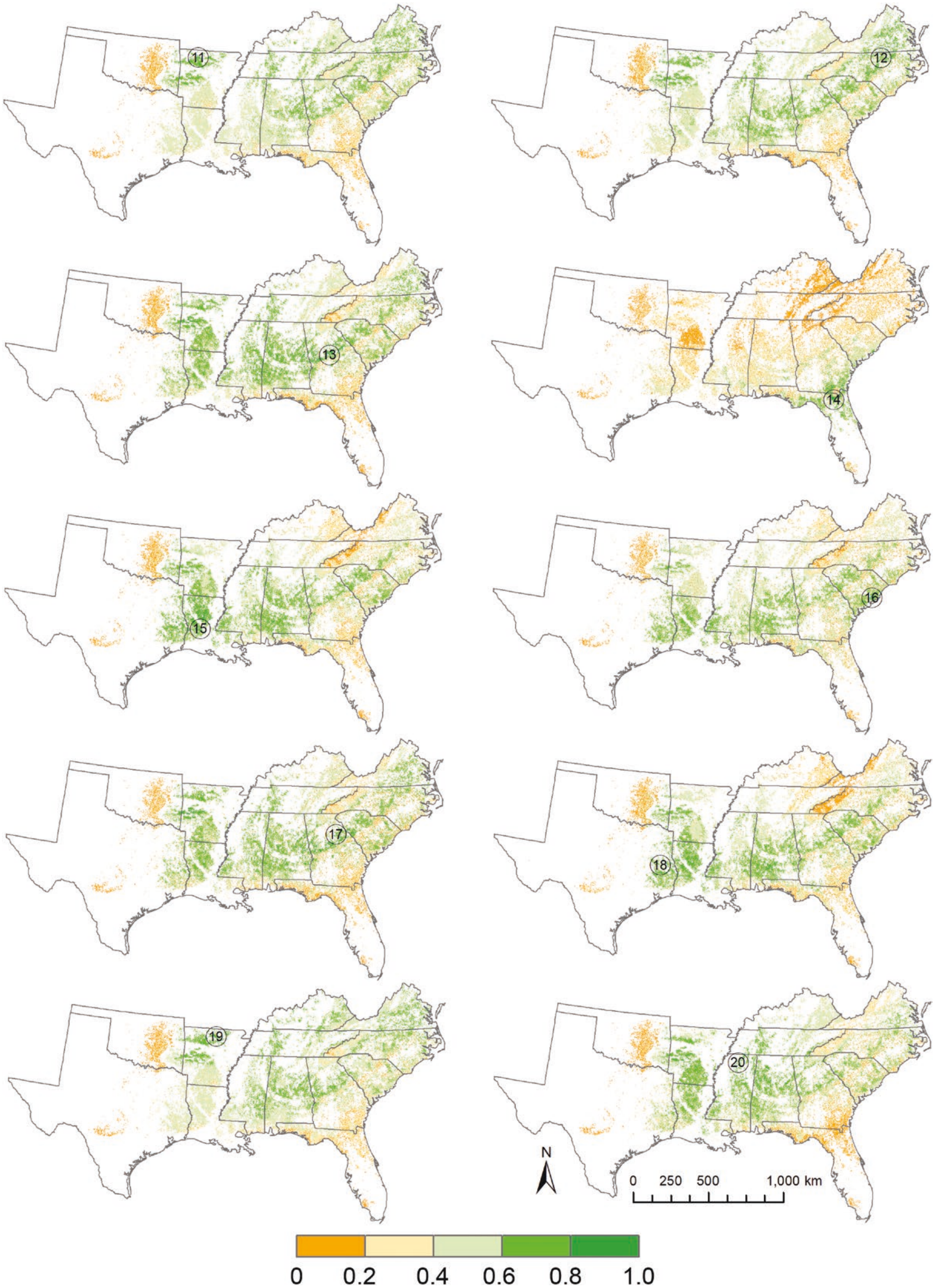

Figure 12 Continued

for other regions of the United States, projected increases are larger for interior areas of the Southeast than for coastal areas of the region (Carter et al. 2018). Projections for future precipitation are less certain than those for temperature increases (Kunkel et al. 2013). Many model projections show only small changes in precipitation with drier conditions in the far southwest of the region and wetter conditions in the far northeast of the region (Kunkel et al. 2013).

The EFRs have some unique advantages that include dedicated research facilities, core budgets, maintenance

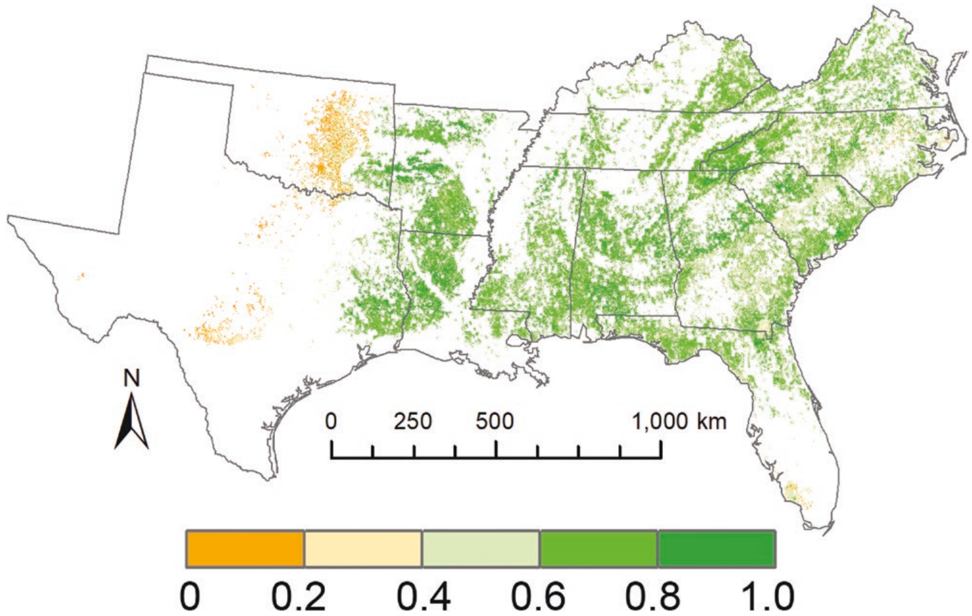

Figure 13 Representativeness of the SRS EFR network assessed with the thirteen variables together. For each pixel, the value indicates the maximum representativeness among the twenty EFRs.

of long-term research and data, involvement of land and resource managers from the FS National Forest System, and support for research across disciplines (Adams et al. 2008). The wealth of long-term datasets spanning up to a century distinguishes EFRs and underscores their value in studying ecological systems. Our societal perspective on the value of forest ecosystems has changed since these EFRs were established. The management of national forests, for example, has shifted from a focus primarily on timber and water to a focus on the management of forest ecosystems, which includes recreation and biodiversity as well as timber and water (Williams 2005). However, to continue to function as an effective EFR network and to address contemporary environmental challenges, it will be vital to define existing conditions across the EFRs and refine and maintain the most important attributes of the network that include data continuity, scientific consistency, baseline data, comparative research, and adaptation to change (e.g., effective methods of data sharing). Future sites in underrepresented regions and continued operation of existing EFRs should consider several factors, including geographic and climate representation and the potential for collaborative cross-site research. In the establishment of new EFRs, other factors that could be important to consider are whether the disturbance and management scenarios are well represented, whether relevant long-term monitoring data already exists for the location to allow for comparison with existing EFRs, and whether funding and personnel are available to maintain the infrastructure needed. Results from this study can provide useful information to offer guidance on the direction of future site selections, on research actions, needs, and programs including new sampling designs, and on scientific infrastructure, tools, and models. The biggest challenges lie in the availability of funding and land. Sufficient and sustained funding will be essential for the successful establishment of a new EFR. Southeastern forests are mostly privately owned and thereby partnerships are likely to be important for the expansion of the network. One practical solution is to identify and incorporate existing university, state, and nonprofit research forests into a larger network of research forests with the EFR network as its backbone.

Conclusions

We assessed how the EFRs represent the variation in climate, ecosystem structure, and ecosystem functions across the southeastern forest region using a variety of gridded data products. The southeastern forest region exhibits large gradients in climate, ecosystem structure, and ecosystem functions. Overall, the existing twenty EFRs managed by the SRS largely represent the distribution of climate (i.e., air temperature, precipitation, shortwave solar radiation, vapor pressure deficit, soil water content, and PDSI), ecosystem structure (i.e., percent tree cover, LAI, tree height), and ecosystem functions (i.e., NPP, ET, AGB, water yield) of the region. The long-term trends in climate, ecosystem structure, and ecosystem functions of the EFRs were generally consistent with those of the southeastern forest region. The representativeness of the mean climate conditions of the region could be improved by establishing EFRs in some parts of the region (e.g., the Appalachian Mountains of Virginia, southern Florida, Oklahoma, and central/northern Texas). Moreover, areas with a percentage of tree cover lower than 45%, LAI lower than 4.5, or tree height lower than 8 m have no EFR representation, indicating that establishing new EFRs in forests with relatively low percentage of tree cover, LAI, or tree height or in young forests could improve the representativeness of the SRS EFR network in terms of ecosystem structure. Establishing EFRs in areas with intermediate and low AGB and WY, such as large parts of South Carolina, Georgia, Oklahoma, and Texas, could improve the representativeness of the EFRs in terms of AGB and water yield. Better understanding and improving the representativeness of the EFRs can help understanding of the past, present, and future changes in southeastern forests in the context of climate change and management. A potential next step would be to identify specific locations for additions to the EFR network to improve its representativeness. One line of work could assess the most efficient way to achieve a certain degree of representativeness—for example, how many more sites are needed to be 95% representative?

This study could provide a framework for how other FS research stations could assess the representativeness of their EFRs. More generally, it could provide a helpful blueprint for assessing the representativeness of any research network (or collection of associated research sites). The findings of this work could help researchers who do work in the SRS EFRs to better understand the geographic context of their work, and to encourage them to think about the limitations of their work and how it could be improved by expanding the EFRs into new locations. For researchers who do not work in these EFRs, the results of this study could encourage them to use the data collected from the network and to apply the resulting research findings to their own work.

Supplementary Material

Supplementary material is available at *Journal of Forestry* online.

Funding

This study was supported by the Southern Research Station of the USDA Forest Service via the Southern Experimental Forests and Ranges Network under Joint Venture Agreement 21-JV-11330180-049, the National Science Foundation (NSF) (Macrosystem Biology & NEON-Enabled Science program: DEB-2017870), and the National Aeronautics and Space Administration (GEDI Science Team: 80NSSC24K0601).

Conflict of Interest

None declared.

Data availability

The data underlying this article will be shared on reasonable request to the corresponding author.

Literature Cited

Abatzoglou, J.T., S.Z. Dobrowski, S.A. Parks, and K.C. Hegewisch. 2018. "TerraClimate, a High-Resolution Global Dataset of Monthly Climate and Climatic Water Balance from 1958-2015." *Scientific Data* 5: 170191. https://doi.org/10.1038/sdata.2017.191.

Adams, M.B., L. Loughry, and L. Plaugher. 2008. *Experimental Forests and Ranges of the USDA Forest Service*. General Technical Report NE-321 Revised. Newtown Square, PA: USDA Forest Service, Northeastern Research Station.

Aguilos, M., B. Mitra, A. Noormets, K. Minick, P. Prajapati, M. Gavazzi, G. Sun, et al. 2020. "Long-Term Carbon Flux and Balance in Managed and Natural Coastal Forested Wetlands of the Southeastern USA." *Agricultural and Forest Meteorology* 288-289: 108022. https://doi.org/10.1016/j.agrformet.2020.108022.

Aguilos, M., G. Sun, N. Liu, Y. Zhang, G. Starr, A.C. Oishi, T.L. O'Halloran, et al. 2024. "Energy Availability and Leaf Area Dominate Control of Ecosystem Evapotranspiration in the Southeastern US." *Agricultural and Forest Meteorology* 349: 109960. https://doi.org/10.1016/j.agrformet.2024.109960.

Blackard, J.A., M.V. Finco, E.H. Helmer, G.R. Holden, M.L. Hoppus, D.M. Jacobs, A.J. Lister, et al. 2008. "Mapping US Forest Biomass Using Nationwide Forest Inventory Data and Moderate Resolution Information." *Remote Sensing of Environment* 112: 1658–1677. https://doi.org/10.1016/j.rse.2007.08.021.

Boggs, J., G. Sun, and S. McNulty. 2016. "Effects of Timber Harvest on Water Quantity and Quality in Small Watersheds in the Piedmont of North Carolina." *Journal of Forestry* 114 (1): 27–40. https://doi.org/10.5849/jof.14-102.

Carter, L., A. Terando, K. Dow, K. Hiers, K.E. Kunkel, A. Lascurain, D. Marcy, M. Osland, and P. Schramm 2018. "Southeast." In *Impacts, Risks, and Adaptation in the United States: Fourth National Climate Assessment, Volume II*, edited by Reidmiller, D.R., C.W. Avery, D.R. Easterling, K.E. Kunkel, K.L.M. Lewis, T.K. Maycock, and B.C. Stewart, 743–808. Washington, DC: US Global Change Research Program. https://doi.org/10.7930/NCA4.2018.CH19.

Chambers, J.Q., J.I. Fisher, H. Zeng, E.L. Chapman, D.B. Baker, and G.C. Hurtt. 2007. "Hurricane Katrina's Carbon Footprint on U.S. Gulf Coast Forests." *Science* 318 (5853): 1107. https://doi.org/10.1126/science.1148913.

Chen, J.M., and T.A. Black. 1992. "Defining Leaf-Area Index for Non-Flat Leaves." *Plant Cell and Environment* 15: 421–429.

Crockett, E.T.H., J.W. Atkins, Q. Guo, G. Sun, K.M. Potter, S. Ollinger, C.A. Silva, et al. 2023. "Structural and Species Diversity Explain Aboveground Carbon Storage in Forests across the United States: Evidence from GEDI and Forest Inventory Data." *Remote Sensing of Environment* 295: 113703. https://doi.org/10.1016/j.rse.2023.113703.

DiMiceli, C., J. Townshend, M. Carroll, and R. Sohlberg. 2021. "Evolution of the Representation of Global Vegetation by Vegetation Continuous Fields." *Remote Sensing of Environment* 254: 112271. https://doi.org/10.1016/j.rse.2020.112271.

Dubayah, R., J.B. Blair, S. Goetz, L. Fatoyinbo, M. Hansen, S. Healey, M. Hofton, et al. 2020. "The Global Ecosystem Dynamics Investigation: High-Resolution Laser Ranging of the Earth's Forests and Topography." *Science of Remote Sensing* 1: 100002. https://doi.org/10.1016/j.srs.2020.100002.

Ficklin, D.L., S.M. Robeson, and J.H. Knouft. 2016. "Impacts of Recent Climate Change on Trends in Baseflow and Stormflow in United States Watersheds." *Geophysical Research Letters* 43 (10): 5079–5088. https://doi.org/10.1002/2016gl069121.

Garland, G., S. Banerjee, A. Edlinger, E.M. Oliveira, C. Herzog, R. Wittwer, L. Philippot, et al. 2021. "A Closer Look at the Functions Behind Ecosystem Multifunctionality: A Review." *Journal of Ecology* 109: 600–613.

Gelaro, R., W. McCarty, M.J. Suarez, R. Todling, A. Molod, L. Takacs, C.A. Randles, et al. 2017. "The Modern-Era Retrospective Analysis for Research and Applications, Version 2 (MERRA-2)." *Journal of Climate* 30 (14): 5419–5454. https://doi.org/10.1175/jcli-d-16-0758.1.

Guldin, J.M. 2009. "The Crossett Experimental Forest—72 Years of Science Delivery in the Silviculture of Southern Pines." In *A Southern Region Conference on Technology Transfer and Extension*, 203–209, edited by Ashton S.F., W.G. Hubbard, H.M. Rauscher. General Technical Report SRS-116. Asheville, NC: USDA Forest Service, Southern Research Station.

Hallgren, S., R. Desantis, and J. Burton. 2012. "Fire and Vegetation Dynamics in the Cross Timbers Forests of South-Central North America." In Proceedings of the 4th Fire in Eastern Oak Forests Conference (GTR-NRS-P-102); 17–19 May 2011; Springfield, MO, USA. Gen. Tech. Rep. NRS-P-102. Newtown Square, PA: U.S. Department of Agriculture, Forest Service, Northern Research Station: 52–66.

Hargrove, W.W., F.M. Hoffman, and B.E. Law. 2003. "New Analysis Reveals Representativeness of the AmeriFlux Network." *Eos, Transactions American Geophysical Union* 84 (48): 529–535.

Hoffman, J., S.G. McNulty, C. Brown, K.D. Dello, P.N. Knox, A. Lascurain, C. Mickalonis, et al. 2023. *Southeast Chapter. National Climate Assessment.*. Washington, DC: United States Global Change Research Program Report.

Kendall, M.G. 1938. "A New Measure of Rank Correlation." *Biometrika* 30 (1/2): 81–93. https://doi.org/10.2307/2332226.

Kumar, J., A.W. Coffin, C. Baffaut, G.E. Ponce-Campos, L. Witthaus, and W.W Hargrove. 2023. "Quantitative Representativeness and Constituency of the Long-Term Agroecosystem Research Network and Analysis of Complementarity with Existing Ecological Networks." *Environmental Management* 72 (4): 705–726. https://doi.org/10.1007/s00267-023-01834-9.

Kunkel, K.E., L.E. Stevens, S.E. Stevens, L. Sun, E. Janssen, D. Wuebbles, C.E. Konrad II, et al. 2013. *Regional Climate Trends and Scenarios for the U.S. National Climate Assessment: Part 2. Climate of the Southeast U.S.*, 103. NOAA Technical Report 142-2, Washington, DC: National Oceanic and Atmospheric Administration, National Environmental Satellite, Data, and Information Service.

Laseter, S.H., J.M. Vose, J.M. Guldin, D.C. Bragg, M.A. Spetich, T.L. Keyser, K.J. Elliott, M.A.S. Sayer, and S.-J.S. Sung. 2018. "Experimental Forests of the Southern Research Station: Highlights of Foundational Silviculture Studies." In Kirschman Julia E., compiler Proceedings of the 19th Biennial Southern Silvicultural Research Conference, 2017 March 14-16, Blacksburg, VA. e-General Technical Report SRS-234. Asheville, NC: USDA Forest Service, Southern Research Station, 149–151.

Li, F., J. Xiao, J. Chen, A. Ballantyne, K. Jin, B. Li, M. Abraha, et al. 2023. "Global Water Use Efficiency Saturation Due to Increased Vapor Pressure Deficit." *Science* 381 (6658): 672–677. https://doi.org/10.1126/science.adf5041.

Liu, N., G.R. Dobbs, P.V. Caldwell, C.F. Miniat, P.V. Bolstad, S. Nelson, and G. Sun. 2020. *Quantifying the Role of State and Private Forest Lands in Providing Surface Drinking Water Supply for the Southern United States*, 405. General Technical Report SRS–248. Asheville, NC: USDA Forest Service, Southern Research Station.

Liu, Y.B., J.F. Xiao, W.M. Ju, G.L. Zhu, X.C. Wu, W.L. Fan, D.Q. Li, et al. 2018. "Satellite-Derived LAI Products Exhibit Large Discrepancies and Can Lead to Substantial Uncertainty in Simulated Carbon and Water Fluxes." *Remote Sensing of Environment* 206: 174–188. https://doi.org/10.1016/j.rse.2017.12.024.

Loftis, D.L. 1990. "A Shelterwood Method for Regenerating Red Oak in the Southern Appalachians." *Forest Science* 36 (4): 917–929. https://doi.org/10.1093/forestscience/36.4.917.

Mann, H.B. 1945. "Nonparametric Tests Against Trend." *Econometrica* 13 (3): 245–259. https://doi.org/10.2307/1907187.

McNulty, S.G. 2002. "Hurricane Impacts on US Forest Carbon Sequestration." *Environmental Pollution* 116: S17–S24. https://doi.org/10.1016/s0269-7491(01)00242-1.

Mu, Q.Z., M.S. Zhao, and S.W. Running. 2011. "Improvements to a MODIS Global Terrestrial Evapotranspiration Algorithm." *Remote Sensing of Environment* 115 (8): 1781–1800. https://doi.org/10.1016/j.rse.2011.02.019.

Munoz-Sabater, J., E. Dutra, A. Agusti-Panareda, C. Albergel, G. Arduini, G. Balsamo, S. Boussetta, et al. 2021. "ERA5-Land: A State-of-the-Art Global Reanalysis Dataset for Land Applications." *Earth System Science Data* 13 (9): 4349–4383. https://doi.org/10.5194/essd-13-4349-2021.

Myneni, R.B., S. Hoffman, Y. Knyazikhin, J.L. Privette, J. Glassy, Y. Tian, Y. Wang, et al. 2002. "Global Products of Vegetation Leaf Area and Fraction Absorbed PAR from Year One of MODIS Data." *Remote Sensing of Environment* 83 (1-2): 214–231. https://doi.org/10.1016/s0034-4257(02)00074-3.

Nippgen, F., B.L. McGlynn, R.E. Emanuel, and J.M. Vose. 2016. "Watershed Memory at the Coweeta Hydrologic Laboratory: The Effect of Past Precipitation and Storage on Hydrologic Response." *Water Resources Research* 52 (3): 1673–1695. https://doi.org/10.1002/2015wr018196.

Oswalt, S.N., W.B. Smith, P.D. Miles, and S.A. Pugh. 2014. *Forest Resources of the United States, 2012: A Technical Document Supporting the Forest Service 2015 Update of the RPA Assessment*, 218. USDA Forest Service General Technical Report WO-91. Washington, DC.

Palmer, W.C. 1965. *Meteorological Drought*. Washington, DC: Research Paper No. 45. US Department of Commerce.

Potapov, P., X.Y. Li, A. Hernandez-Serna, A. Tyukavina, M.C. Hansen, A. Kommareddy, A. Pickens, et al. 2021. "Mapping Global Forest Canopy Height Through Integration of GEDI and Landsat Data." *Remote Sensing of Environment* 253: 112165. https://doi.org/10.1016/j.rse.2020.112165.

Running, S.W., R.R. Nemani, F.A. Heinsch, M.S. Zhao, M. Reeves, and H. Hashimoto. 2004. "A Continuous Satellite-Derived Measure of Global Terrestrial Primary Production." *Bioscience* 54 (6): 547–560. https://doi.org/10.1641/0006-3568(2004)054[0547:acsmog]2.0.co;2.

Rustad, L., M.B. Adams, S.F. Dymond, M. Gregory, and G.F. Miniat. 2023. "Perspectives on the Contributions of Women to the Hydrologic Sciences and their Changing Demographics at USDA Forest Service Experimental Forests and Ranges." *Journal of Hydrology* 621: 129469. https://doi.org/10.1016/j.jhydrol.2023.129469.

Sokal, R.R., and F.J. Rohlf. 1995. *Biometry: The Principles and Practice of Statistics in Biological Research*, 3rd ed, 539. New York: W.H. Freeman.

Stein, B.A., L.S. Kutner, and J.S. Adams, editors. 2000. *Precious Heritage: The Status of Biodiversity in the United States*, 416. New York: Oxford University Press.

Stine, P.A. 2016. *Forest Service Research and Development: Strategic Vision for the Experimental Forests and Ranges Network*, 198. General Technical Report PNW-GTR-935. Portland, OR: USDA Forest Service, Pacific Northwest Research Station.

Sun, G., P. Caldwell, A. Noormets, S.G. McNulty, E. Cohen, J.M. Myers, J.C. Domec, et al. 2011. "Upscaling Key Ecosystem Functions across the Conterminous United States by a Water-Centric Ecosystem Model." *Journal of Geophysical Research, Biogeosciences* 116: G00J05. https://doi.org/10.1029/2010JG001573.

Sun, G., S.G. McNulty, J. Lu, D.M. Amatya, Y. Liang, and R.K. Kolka. 2005. "Regional Annual Water Yield from Forest Lands and Its Response to Potential Deforestation Across the Southeastern United States." *Journal of Hydrology* 308 (1-4): 258–268. https://doi.org/10.1016/j.jhydrol.2004.11.021.

Sun, G., S.G. McNulty, J.A. Moore Myers, and E.C. Cohen. 2008. "Impacts of Multiple Stresses on Water Demand and Supply across the Southeastern United States." *Journal of the American Water Resources Association* 44: 1441–1457.

Swank, W.T., J.M. Vose, and K.J. Elliott. 2001. "Long-Term Hydrologic and Water Quality Responses Following Commercial Clearcutting of Mixed Hardwoods on a Southern Appalachian Catchment." *Forest Ecology and Management* 143 (1-3): 163–178. https://doi.org/10.1016/s0378-1127(00)00515-6.

Swift, L.W. Jr. 1986. "Filter Strip Widths for Forest Roads in the Southern Appalachians." *Southern Journal of Applied Forestry* 10 (1): 27–34. https://doi.org/10.1093/sjaf/10.1.27.

USDA Forest Service. 2023. "Experimental Forests and Ranges." Updated July 4, 2023 https://www.fs.usda.gov/research/forestsandranges.

Wang, X.F., J.F. Xiao, X. Li, G.D. Cheng, M.G. Ma, G.F. Zhu, M.A. Arain, et al. 2019. "No Trends in Spring and Autumn Phenology During the Global Warming Hiatus." *Nature Communications* 10: 2389. https://doi.org/10.1038/s41467-019-10235-8.

Williams, A.P., B.I. Cook, J.E. Smerdon, D.A. Bishop, R. Seager, and J.S. Mankin. 2017. "The 2016 Southeastern US Drought: An Extreme Departure From Centennial Wetting and Cooling." *Journal of Geophysical Research-Atmospheres* 122: 10888–10905.

Williams, G.W. 2005. *The USDA Forest Service: the First Century. FS-650*, 156. Washington, DC: USDA Forest Service.

World Resources Institute. 2010. "Southern Forests for the Future." http://www.wri.org.

Xiao, J.F., Q.L. Zhuang, B.E. Law, D.D. Baldocchi, J.Q. Chen, A.D. Richardson, J.M. Melillo, et al. 2011. "Assessing Net Ecosystem Carbon Exchange of U.S. Terrestrial Ecosystems by Integrating Eddy Covariance Flux Measurements and Satellite Observations." *Agricultural and Forest Meteorology* 151: 60–69. https://doi.org/10.1016/j.agrformet.2010.09.002.